Less surface sea ice melt in the CESM2 improves Arctic sea ice simulation with minimal non-polar climate impacts

Jennifer E. Kay[1,2], Patricia DeRepentigny[1,3], Marika M. Holland[4], David A. Bailey[4], Alice K. DuVivier[4], Ed Blanchard-Wrigglesworth[5], Clara Deser[4], Alexandra Jahn[1,3], Hansi Singh[6], Madison M. Smith[5], Melinda A. Webster[7], Jim Edwards[4], Sun-Seon Lee[8,9], Keith B. Rodgers[8,9], and Nan Rosenbloom[4]

[1]Department of Atmospheric and Oceanic Sciences, University of Colorado, Boulder, CO
[2]Cooperative Institute for Research in Environmental Science, University of Colorado, Boulder, CO
[3]Institute of Arctic and Alpine Research, University of Colorado, Boulder, CO
[4]National Center for Atmospheric Research, Boulder, CO
[5]University of Washington, Seattle, WA
[6]University of Victoria, British Columbia, Canada
[7]University of Alaska Fairbanks, AK
[8]Center for Climate Physics, Institute for Basic Science, Busan, South Korea
[9]Pusan National University, Busan, South Korea

Corresponding author: Jennifer E. Kay (jennifer.e.kay@colorado.edu)
Submitted to *Journal of Advances in Modeling Earth Systems*
June 29, 2021

Publication Units: 6478 words *(~13 PU, each PU is 500 words),* 15 Figures. Total PU = 28.

Key Points (limit 140 characters each):

- Decreasing surface melt decreases late-summer Arctic sea ice cover biases and delays transition to an ice-free Arctic Ocean
- Internal variability limits value of sea ice trends and sea ice sensitivity as metrics to constrain model performance
- Increasing sea ice thickness and area has negligible impacts on non-polar climate and climate change

Abstract (Limit 250 words, 249 now)

This study isolates the influence of sea ice mean state on pre-industrial climate and transient 1850-2100 climate change within a fully coupled global model: The Community Earth System Model version 2 (CESM2). The CESM2 sea ice model is modified to increase surface albedo, reduce surface sea ice melt, and increase Arctic sea ice thickness and late summer cover. Importantly, increased Arctic sea ice in the modified model reduces a well-known present-day late-summer ice cover bias. Of interest to coupled model development, this bias reduction is realized without degrading the global model simulation including top-of-atmosphere energy imbalance, surface temperature, surface precipitation, and major modes of climate variability. The influence of sea ice mean state on transient 1850-2100 climate change is compared within a large initial condition ensemble framework. Despite similar global warming, the modified model with thicker Arctic sea ice than CESM2 has a delayed and more realistic transition to a seasonally ice free Arctic Ocean. Differences in transient climate change between the modified model and CESM2 are challenging to detect due to large internally generated climate variability. In particular, two common sea ice benchmarks - sea ice sensitivity and sea ice trends - are of limited value for contrasting model performance. More broadly, these results show the importance of a reasonable initial Arctic sea ice state when simulating the transition to an ice-free Arctic Ocean in a warming world. Additionally, this work highlights the need for and value of large initial condition ensembles for credible model-to-model and observation-model comparisons.

Plain Language Summary (200 word limit, 199 now)

Satellite observations available from 1979 to present show dramatic Arctic sea ice loss. As a result, projecting when the Arctic Ocean may become ice free and the resulting impacts is of broad interest to those living in the Arctic and beyond. Climate models are the main tool for making such future projections. Yet, projecting sea ice loss is hard because it is affected by multiple factors that are often impossible to disentangle including physical processes, unpredictable climate variability, and differences in climate drivers. Unique to this work, we analyze the influence of the initial amount of sea ice while also controlling for all other confounding factors such as the amount of global warming and unpredictable climate variability. Our work demonstrates that under similar global warming, the initial amount of Arctic sea ice affects the timing of an ice-free Arctic Ocean. Specifically, simulations with more sea ice initially transition to an ice-free Arctic Ocean later. Notably, the initial amount of sea ice has little influence on 20-year Arctic sea ice trends. We also found initial sea ice amounts and the timing towards an ice-free Arctic have negligible influence on warming, precipitation, and sea level pressure outside of the polar regions.

1. Motivation and Study Goals

Satellite-observed Arctic Ocean sea ice cover decreases over the last few decades are a visible manifestation of human-caused climate change. Earth system models cannot reproduce this observed ice loss with natural forcing alone (e.g., Kirchmeier-Young et al. 2017, Kay et al. 2011). While models can reproduce the sign of observed multi-decadal Arctic sea ice area trends, these same models exhibit differing Arctic sea ice loss rates and timing (Swart et al. 2015, SIMIP Community 2020). Why do Arctic sea ice loss rates differ between model simulations? Given similar global warming, two factors are important to consider. First, mean state matters: models with thicker Arctic sea ice tend to exhibit less ice area loss but more ice volume loss than models with thinner sea ice (e.g., Massonnet et al. 2018, Holland et al. 2010, Bitz 2008). Second, internally generated climate variability influences differences in Arctic sea ice loss timing and trends (e.g., SIMIP Community 2020, Jahn et al. 2016, Swart et al. 2015, Notz 2015, Wettstein and Deser 2014, Kay et al. 2011). In fact, recent work emphasizes that internal variability dominates over emissions scenario in affecting projected sea ice loss over the upcoming 2-3 decades, including the timing of the first ice-free Arctic Ocean in late summer (e.g., Bonan et al., 2021, DeRepentigny et al. 2020, Jahn 2018, Sigmond et al. 2018).

Sea ice mean state influences transient sea ice response to climate forcing. Indeed, mean sea ice thickness has well-known foundational influences on vertical sea ice thermodynamics (Bitz and Roe 2004, Holland et al. 2006). The two dominant feedbacks internal to sea ice – the positive sea ice albedo feedback and the negative ice-thickness growth feedback – strengthen when sea ice thins. Sea ice loss in models with a wide range of complexities show the importance of sea ice mean thickness to thermodynamic sea ice growth and loss. In addition, mean sea ice thickness affects sea ice variability and predictability. When sea ice thins, ice area variability increases, ice thickness variability decreases, and predictor relationships change in location, nature, and magnitude (e.g., Holland et al. 2019, Mioduszewski et al. 2018, Swart et al. 2015, Holland and Stroeve 2011, Blanchard Wrigglesworth et al. 2011, Kay et al. 2011).

While the importance of sea ice mean state is uncontroversial, the potential to constrain the mean state and reduce projection uncertainty remains unclear. Recent work by Massonnet et al. (2018) used regression to quantify the relationship between Arctic sea ice mean state and transient loss rates in a multi-model ensemble (Coupled Model Intercomparison Project version 5 (CMIP5), Taylor et al. 2012). While the relationships between mean state and linear changes in March sea ice volume and September sea ice area were weak, they were statistically significant. The study arrived at two important conclusions. First, given the importance of mean state and in particular sea ice thickness mean state, models with a biased mean sea ice thickness should be questioned and potentially not used for future projections. Second, it is currently not possible to observationally constrain the sea ice thickness mean state due to the lack of long-term and reliable observations. This second conclusion is especially striking, is consistent with a recent community analysis that questioned the accuracy of sea ice thickness observations (e.g., SIMIP Community 2020), and leaves many open questions: 1) How reliable is reliable enough? 2) How long of an observational record is needed? 3) Does tuning to observed sea ice extent/area help constrain sea ice thickness? Model tuning is necessary (e.g., Mauritsen et al. 2012), and best accomplished when constrained by available observations, especially when the mean state influences transient response as is the case for sea ice.

Even if the sea ice mean state can be observationally constrained, internally generated climate variability obscures the influence of the mean state on the transient sea ice response. Having many realizations that show the same response increases confidence that a signal results from a sea ice thickness difference and not from internally generated climate variability. As a result, large initial-condition ensembles are needed to quantify the influence of mean sea ice state on sea ice projections. While such ensembles are becoming more standard practice and more broadly available with CMIP-class models (e.g., Deser et al. 2020), sensitivity tests using large ensembles as a control are rare. In particular, a targeted experiment that isolates the influence of sea ice mean state on climate change and variability in a CMIP-class model with a large ensemble has not been done.

In this study, we build on previous work by isolating the influence of the sea ice mean state on climate. We focus on two research questions:

1) Does pre-industrial sea ice mean state influence the rate and timing of transient anthropogenically forced sea ice change? In particular, does thicker Arctic sea ice in the pre-industrial mean state lead to slower sea ice loss and a later transition to seasonally ice-free conditions in transient projections for the 21st century?
2) What is the impact of pre-industrial sea ice mean state on key global climate variables (surface temperature, precipitation, and sea level pressure)? Specifically, can we detect the influence of sea ice mean state on pre-industrial climate and 1850-2100 transient climate change and variability in both polar and non-polar regions?

To answer our research questions, we modify the sea ice model within an earth system model to increase surface albedo, reduce surface melt, and increase the mean state sea ice. We then quantify the influence of the sea ice mean state differences on mean and transient climate change using a large initial condition ensemble as a control. Working within this numerical simulation framework, we can isolate differences in transient projections that arise from sea ice mean state alone. While we present results from both poles, we focus more on the Arctic where the parameter changes have a larger impact and reduce a model bias. We find that with thicker sea ice, the transition to an ice-free Arctic Ocean is delayed. In addition, the impacts of sea ice tuning on non-polar climate are small. While our results rely on one model, our analysis provides guidance for future modeling development efforts, especially those that hope to optimize their simulation of transient Arctic sea ice loss.

2. Methods

2.1 Model simulations and comparison strategies

We use a well-documented state-of-the-art global climate model: the Community Earth System Model version 2 (CESM2) with the Community Atmosphere Model version 6 (CAM6) (Danabasoglu et al. 2020). CESM2-CAM6, hereafter shortened to simply CESM2, is an attractive model to use for two reasons. First, comprehensive simulations exist for CESM2 as a part of the Coupled Model Intercomparison Project version 6 (CMIP6) (Eyring et al. 2016) and a recently released large initial-condition ensemble, hereafter referred to as the CESM2-LE (Rodgers et al. 2021). Second, CESM2 has a mean state Arctic sea ice bias. When compared to present-day observations, CESM2 has insufficient late summer Arctic sea ice cover, a bias that has been attributed to the sea ice being too thin (Danabasoglu et al. 2020 Figure 17g, DuVivier et al. 2020). The consequences of this CESM2 thin Arctic sea ice bias for transient sea ice change have been documented in DeRepentigny et al. (2020). For example, the 11 CESM2 CMIP6 transient historical simulations have ice-free late summer conditions in the Arctic as early as 2010, which is inconsistent with satellite observations even when accounting for internal variability.

Inspired to remedy the CESM2 thin Arctic sea ice bias and assess its impact on the global climate system, we created CESM2-lessmelt. CESM2-lessmelt is identical to CESM2 except for two parameter modifications made within the thermodynamics of the sea ice model. The sea ice model in CESM2 (CICE 5.1.2; Hunke et al. 2015) uses a multiple-scattering Delta-Eddington radiative transfer parameterization which relies on the specification of inherent optical properties (Briegleb and Light 2007). These optical properties can be adjusted to change the albedo of snow-covered sea ice. In CESM2-lessmelt, we changed the r_snw parameter such that the dry snow grain radius decreases from 187.5 μm to 125 μm, thereby increasing the albedo of snow on sea ice. In addition, we changed the dt_mlt parameter such that the melt onset temperature increases by 0.5 °C from -1.5 °C to -1.0 °C. This melt onset temperature determines when the snow grain radius starts to grow from a dry snow value to a melting snow value. Both CESM2-lessmelt parameter changes were implemented to increase snow albedo, reduce sea ice melt, and increase the mean state sea ice thickness. Both parameter changes were made globally and thus affect sea ice in both hemispheres. Finally, both parameter changes are within the observational uncertainty provided by in situ observations from Surface Heat Budget of the Arctic Ocean (SHEBA).

In this work, we compare simulations with constant pre-industrial control climate conditions. For CESM2, we use the multi-century CMIP6 1850 pre-industrial control run. For CESM2-lessmelt, we ran a 550-year-long CESM2-lessmelt 1850 pre-industrial control run. The CESM2-lessmelt control was branched from year 881 of the CESM2 CMIP6 control. As a sanity check, we assessed global metrics of energy conservation and climate stability in the CESM2-lessmelt control and compared it to the CESM2 control during overlapping years. The global mean surface temperature is 0.16 K lower in CESM2-lessmelt (288.18 K) than in CESM2 (288.34 K). The top-of-model energy imbalance in both models is small: -0.02 Wm^{-2} for CESM2-lessmelt and 0.07 Wm^{-2} for CESM2. Both models exhibit negligible drift in their global mean surface temperature and top-of-model energy imbalance. Thus, both CESM2 model versions meet basic energy conservation and stability criteria for global coupled modeling science.

In addition to pre-industrial control comparisons, we also compare simulations of 1850-2100 transient climate change under the same CMIP6 forcing. For CESM2, we use the first 50 ensemble members of the CESM2-LE. As described in Rodgers et al. (2021), members 1-50 share the same transient CMIP6 forcing: historical (1850-2014) and the SSP3-7.0 future scenario (2015-2100) (O'Neil et al. 2016). For CESM2-lessmelt, we ran a 4-member mini ensemble using the same historical and SSP3-7.0 CMIP6 forcing as CESM2-LE members 1-50. The first CESM2-lessmelt ensemble member started at year 1181 of the CESM2-lessmelt 1850 pre-industrial control run and was run from 1850 to 2100. Three additional CESM2-lessmelt ensemble members were run from 1920 to 2100 with initial conditions from the first CESM2-lessmelt ensemble member perturbed by round-off (10^{-14} K) differences in air temperature.

As all transient ensemble members analyzed in this work share the same forcing, we assume each ensemble member is an equally likely estimate of the transient climate response. This "equally likely" assumption is justified in the Supporting Information (Text S1, Figures S1-S5). This assumption enables us to statistically quantify differences between CESM2-LE and CESM2-lessmelt. Given the differences in ensemble size, we use bootstrapping to statistically assess when the 4 CESM2-lessmelt ensemble members are distinct from the first 50 members of the CESM2-LE. Bootstrapping, or randomly resampling to generate statistics, requires no distribution assumptions.

Finally, it is important to note a feature of all transient model simulations analyzed here. Namely, the CMIP6 historical forcing includes a stark increase in the inter-annual variability of biomass burning emissions during the satellite era of wildfire monitoring 1997-2014 (Fasullo et al. 2021, DeRepentigny et al. 2021). This discontinuity leads to excessive surface warming in the northern hemisphere extratropics (Fasullo et al. 2021). It also contributes to 1997-2010 Arctic sea ice loss followed by a 2010-2025 Arctic sea ice recovery (DeRepentigny et al. 2021). While several CMIP6 models show impacts from this discontinuity, the CESM2 has a particularly pronounced response. In this work, we use this discontinuity as an opportunity to assess the influence of sea ice mean state on the sea ice response to a short-term radiative forcing.

3. Results

3.1. Pre-industrial sea ice in CESM2 and CESM2-lessmelt

Comparison of pre-industrial sea ice volume and cover monthly mean values show CESM2-lessmelt has more sea ice than CESM2 in both hemispheres (Figure 1). In the Arctic, sea ice volume in CESM2-lessmelt exceeds that in CESM2 during all months (**Figure 1a**). In contrast, Arctic sea ice cover differences have a distinct seasonal cycle with large late summer differences and small winter differences (**Figure 1b**). In the Antarctic, CESM2-lessmelt has larger sea ice cover and volume than CESM2 in all months (**Figure 1c,d**). Monthly mean volume differences between CESM2 and CESM2-lessmelt are larger in the Arctic (30% greater in CESM2-lessmelt) than in the Antarctic (8% greater in CESM2-lessmelt).

Spatially, the largest sea ice cover differences occur at the sea ice edge where/when the sea ice can expand/contract without influence of land barriers and ocean circulation. At the late summer seasonal minimum, the CESM2-lessmelt sea ice edge expands equatorward at the sea ice margin in both hemispheres (**Figure 2**). Yet, this late summer expansion in CESM2-lessmelt is not zonally uniform. In the Arctic, the largest late summer ice concentration increases in CESM2-lessmelt occur North of Russia in the East Siberian Sea (**Figure 2b**). In contrast, only modest late summer sea ice expansion happens in the North Atlantic. In the Antarctic, the largest magnitude late summer sea ice concentration expansion equatorward occurs off the coast east of the Weddell Sea (**Figure 2d**). Changes in late-summer Antarctic sea ice concentration are otherwise small, likely due to the lack of sea ice at the seasonal minimum. At the seasonal maximum in late winter, Arctic concentrations differences are small due to the land barriers and the ocean heat convergence that controls the sea ice edge (**Figure 3a-b;** Bitz et al. 2005). In the Antarctic, the late winter sea ice edge has a zonally non-uniform response with some regions exhibiting sea ice concentration increases and others exhibiting sea ice concentration decreases

(**Figure 3c-d**). In particular, there is less sea ice cover in CESM2-lessmelt than in CESM2 in the Ross Sea. Non-zonally asymmetric sea ice differences demonstrate the importance of both thermodynamic and dynamic responses to the sea ice parameter changes made in CESM2-lessmelt.

Sea ice thickness comparisons are also of interest, especially in the Arctic where thicker ice in late winter can lead to less late summer sea ice loss. Unlike the concentration differences that manifested at the sea ice edge, sea ice thickness differences at the late winter seasonal maximum occur throughout the sea ice pack (**Figure 4**). Late-winter sea ice thicknesses are at least 0.5 m greater in CESM2-lessmelt than in CESM2 throughout the central Arctic basin (**Figure 4b**). Antarctic sea ice thickness differences are much smaller, generally less than 0.25 meters (**Figure 4d**). The largest differences in the Antarctic occur off the west side of the Antarctic Peninsula in the Bellingshausen Sea.

To quantify processes underlying the mean state differences between the two CESM2 model variants, we next compare their sea ice mass tendencies. In addition to analyzing the total sea ice mass tendency, we also decompose this total tendency into contributions from dynamic and thermodynamic processes. Dynamic mass tendencies result from advection of ice into or out of a grid cell. Thermodynamic mass tendencies result from the sum of basal ice growth, ice growth in supercooled open water, transformation of snow to sea ice, surface melting, lateral melting, basal melting and evaporation/sublimation. See DuVivier et al. (2020), Singh et al (2021), and Bailey (2021) for more information about these diagnostics including their application to evaluate CESM2 sea ice. Consistent with a balanced mean state and negligible model drift, the annual mean tendency terms differences are small (not shown). Yet, substantial differences in the sea ice mass tendency terms occur during both the growth season and the melt season in both hemispheres in response to the parameter changes made in CESM2-lessmelt.

Arctic sea ice mass tendency diagnostics show CESM2 and CESM2-lessmelt differences result from both thermodynamics and dynamics (Figure 5). During the melt season, CESM2-lessmelt has less Arctic thermodynamic sea ice mass loss than CESM2. This thermodynamic sea ice mass loss difference is consistent with a higher snow albedo in CESM2-lessmelt than in CESM2. CESM2-lessmelt also has less thermodynamic Arctic sea ice mass gain than CESM2 during the growth season due to the negative ice-thickness growth feedback (Bitz and Roe, 2004). These opposing seasonal influences on thermodynamic tendency terms are consistent with thicker Arctic sea ice in CESM2-lessmelt than in CESM2. Dynamical sea ice tendency terms dominate at the sea ice edge and during the growth season. With its thicker sea ice, CESM2-lessmelt has more ice export out of and more ice transport within the Arctic basin than CESM2. When more ice is moved into a region where sea ice can melt, thermodynamic mass tendencies and dynamic mass tendencies compensate.

We next evaluate sea ice mass tendencies for CESM2 and CESM2-lessmelt in the Antarctic (Figure 6). Positive dynamic mass tendencies increase sea ice away from the Antarctic coast in all seasons. This dynamically driven sea ice mass increases result from wind-driven transport of sea ice away from the Antarctic coast. During the growth season, thermodynamically-driven sea ice mass gains occur near the coast, which in turn increases dynamically-driven sea ice mass gains away from the coast. When compared to CESM2, CESM2-lessmelt has more dynamical mass gain associated with this wind-driven sea ice advection in all seasons. During the melt season, sea ice mass loss due to thermodynamics is less in CESM2-lessmelt than in CESM2. Yet, the growth season in the Antarctic differs from that in the Arctic. Unlike in the Arctic, the Antarctic has little multi-year ice and thus no negative ice-thickness growth feedback. Also unlike the Arctic, the Antarctic gains mass through snow-ice formation.

3.2. Influence of sea ice tuning on pre-industrial global climate

Overall, CESM2-lessmelt and CESM2 have statistically significant differences in surface air temperature, precipitation, and sea level pressure at both poles (Figure 7). In contrast, impacts on non-polar climate are small and not statistically significant. Where CESM2-lessmelt has more sea ice than CESM2, the Arctic and Antarctic surface are both cooler in CESM2-lessmelt than in CESM2, especially in non-summer seasons. Demonstrating the importance of sea ice to polar surface temperatures, Ross Sea air temperatures increased in CESM2-lessmelt when compared to CESM2, consistent with sea ice concentration and thickness decreases from CESM2-lessmelt to CESM2 in this region (**Figure 3d, Figure 4d**). Generally speaking, precipitation differences between CESM2 and CESM2-lessmelt followed surface temperature differences. The relatively cooler CESM2-lessmelt atmosphere converges less moisture and has less precipitation, especially in Fall in the Arctic. Despite this precipitation reduction, CESM2-lessmelt has 10% more snow on Arctic sea ice in spring than CESM2, which is in better agreement with observations (Webster et al., 2021). Overall, polar sea level pressure differences are generally small and not statistically significant. One notable exception are statistically significant sea level pressure differences between CESM2 and CESM2-lessmelt during Arctic Fall, including the well-known atmospheric circulation response to boundary layer thermal forcing (e.g., Deser et al. 2010). Here, boundary layer cooling in CESM2-lessmelt leads to a local high SLP response in autumn (baroclinic vertical structure).

In addition to mean climate state, we also assessed climate variability differences arising from the different sea ice mean states in CESM2 and CESM2-lessmelt. In brief, pre-industrial climate variability differences between the multi-century CESM2 and CESM2-lessmelt pre-industrial control runs are small and not statistically significant. Major modes of climate variability, such as those plotted in the Climate Variability Diagnostics Package (Phillips et al 2020), are unchanged between CESM2 and CESM2-lessmelt pre-industrial control runs. Similarly, differences in inter-annual seasonal surface temperature, sea level pressure, and precipitation standard deviations are small and not statistically significant (**Figure S6**).

3.3. Transient (1850-2100) sea ice evolution in CESM2 and CESM2-lessmelt

Present-day (1979-2014) monthly hemispheric mean differences (**Figure 8**) resemble corresponding pre-industrial control differences (**Figure 1**). In the Arctic, CESM2-lessmelt has more present-day sea ice volume than CESM2 in every month (**Figure 8a**). Moreover, CESM2-lessmelt also has more present-day Arctic sea ice cover than CESM2 in all months, with the largest differences during the melt season and especially in late summer (**Figure 8b-c**). Overall, the Arctic sea ice mean state is closer to observations in CESM2-lessmelt than in CESM2. Of particular note, additional present-day late summer Arctic sea ice cover brings CESM2-lessmelt closer to observations than CESM2. While present-day hemispheric multi-decadal Arctic sea ice volume observations are not available (Massonnet et al. 2018), reductions in late-summer sea ice cover biases are consistent with CESM2-lessmelt having more realistic sea ice volume than CESM2. Like in the Arctic, present-day Antarctic sea ice differences between CESM2 and CESM2-lessmelt are also qualitatively similar to the pre-industrial control (**Figure S7**). But unlike in the Arctic, both CESM2 variants have substantial Antarctic mean state biases without consistent bias reduction from CESM2 to CESM2-lessmelt. Given similar Antarctic sea ice biases, relatively modest Antarctic mean state sea ice changes, and the inability of CESM2 and CESM2-tuned ice to reproduce observed Antarctic sea trends (**Figure S8**), we focus on the Arctic for the remainder of the transient sea ice comparisons.

Arctic maps reveal that the sea ice in CESM2 and CESM2-lessmelt evolves differently from the present-day into the 21st century (Figure 9). While both CESM2 and CESM2-lessmelt have their greatest present-day (1979-2014) late winter sea ice thicknesses and late summer sea ice concentrations north of Greenland and the Canadian Archipelago, CESM2-lessmelt has more sea ice throughout much of the Arctic Ocean than CESM2 (**Figure 9a-d**). Notably, September Arctic sea ice concentrations are substantially greater in CESM2-lessmelt than in CESM2 (**Figure 9c**). Equally important, the present-day March sea ice is 0.5+ meters thicker in CESM2-lessmelt than in CESM2 over most of the central Arctic Ocean (**Figure 9d**). By 2030-2049, Arctic sea ice differences between CESM2-lessmelt and CESM2 remain for late-summer September concentration but are small for late winter March thickness (**Figure 9e-f**). Large 2030-2049 late summer ice cover differences occur because despite starting the melt season with similar March sea ice thickness distributions, less melt occurs in CESM2-lessmelt than in CESM2. This difference in 2030-2049 summer melt is consistent with higher albedo in CESM2-lessmelt than in CESM2. By 2050-2069, CESM2 and CESM2-lessmelt have similar small September sea ice concentrations (**Figure 9g**) . Consistent with a transition to a seasonally ice-free Arctic, March sea ice thicknesses are also similar in 2050-2069 over much of the Arctic Ocean (**Figure 9h**). In fact, the only regions where 2050-2069 differences between CESM2-lessmelt and CESM2 persist are along the coast of Northern Greenland and the far North Eastern portions of the Canadian archipelago.

While ensemble means provide the most robust assessment of the differences in CESM2 and CESM2-lessmelt, ensemble mean values are not physically realized quantities, mute internal variability, and thus should not be compared as equals with observed timeseries and trends. Instead, each individual CESM2-LE or CESM2-lessmelt ensemble member's time evolution should be treated as equally likely and the observations should be treated as the single real world ensemble member. Consistent with time-averaged ensemble mean comparisons (**Figure 8**), September Arctic sea ice extent in all four CESM2-lessmelt ensemble members (**Figure 10b**) is a better match to 1979-2020 observations than any of the 50 CESM2-LE ensemble members (**Figure 10a**). Up until ice-free conditions are reached, CESM2-lessmelt ensemble members have more September sea ice extent than almost all of the CESM2-LE ensemble members. Unlike sea ice amount, 20-year linear trends in September Arctic sea ice in CESM2-LE, CESM2-lessmelt, and observations largely overlap (**Figure 10c)**. In other words, CESM2-lessmelt and CESM2-LE trends are both consistent with observed trends. Due to ensemble size differences, the spread in CESM2-lessmelt trends is smaller than the spread in CESM2-LE trends. Thus, even though CESM2-lessmelt trends are more negative than observed trends with end dates of 2001-2006, this may simply be the consequence of ensemble size differences. As introduced in section 2.1 and in DeRepentigny et al. (2021), the individual ensemble members show sea ice loss accelerates around the turn of the 21st century and then the sea ice recovers in the early 21st century due to the prescribed biomass burning emissions in CMIP6 forcing.

Continuing with the equally likely framework in mind, we next assess common metrics used for sea ice model evaluation: sea ice sensitivity and the timing of a seasonally

ice-free Arctic (Figure 11). These metrics illustrate the challenge of large internally driven variability for differentiating between CESM2-lessmelt and CESM2-LE and comparing them to observations. For sea ice sensitivity per ton of cumulative anthropogenic CO_2 emissions, both the observations and the CESM2-lessmelt ensemble members lie almost entirely within the spread of the first 50 CESM2-LE members (**Figure 11a**). In contrast, the sea ice sensitivity per global mean warming appears larger in CESM2-lessmelt with three out of four ensemble members outside of the spread of the CESM2-LE (**Figure 11b**). That said, the spread in CESM2-LE sea ice sensitivity values measured with respect to CO_2 and global mean warming is large and humbling. Assuming any individual ensemble member is equally likely, the large spread in sea ice sensitivity metrics shows they are not strong observational constraints and provide limited value as a model comparison metric, especially when ensemble size is small.

Internal variability also has a strong imprint on the timing of a first seasonally ice-free Arctic Ocean. Indeed, the CESM2-LE exhibits a 38 year spread in this metric with years ranging from 2007 to 2045 (**Figure 11c**). While the spread in the CESM2-lessmelt first ice-free Arctic year is small (2041 to 2057), the 4 CESM2-lessmelt first ice-free years barely overlap with the 50 CESM2-LE first ice-free years. Bootstrapping the CESM2-LE ice-free dates shows the two distributions are statistically different at the 95% confidence level. In other words, the thicker and more extensive Arctic sea ice in CESM2-lessmelt delays the timing of an ice free Arctic when compared to CESM2-LE. While the delay of the first ice-free Arctic is statistically significant, the large internally generated variability still limits its predictability by decades. The spread in ice-free years in the first 50 members of the CESM2-LE is made especially large and early by the accelerated sea ice decline associated with the CMIP6 biomass burning emissions (DeRepentigny et al. 2021).

We next use ensemble means to quantify forced response differences between CESM-LE and CESM2-lessmelt (Figure 12). To make consistent forced response comparisons, we bootstrap the 50 CESM2-LE members to generate statistics that are consistent with ensembles with only four members. With these bootstrapped values, we can statistically assess when CESM2-lessmelt and CESM2-LE differ while accounting for differences in ensemble size. For example, if the CESM2-lessmelt ensemble mean lies outside of the 95% confidence limits of sample statistics generated randomly by selecting 4 members of the CESM2-LE many times (here 1,000 times), the forced response differences are statistically significant. Comparing the ensemble means consistent with four ensemble members, we find that CESM2-lessmelt has more September sea ice extent (**Figure 12a**) and more March sea ice volume (**Figure 12b**). Interestingly, twenty-year trends in September sea ice extent and March sea ice volume are statistically indistinguishable in CESM2-lessmelt and CESM2-LE with the exception of three periods (**Figure 12c-d**). The first exception is for the period with trend end dates ~2010 during the biomass burning forcing discontinuity. During this time period, the CESM2-lessmelt has less negative sea ice extent trends and more negative sea ice volume trends than the CESM2-LE. This first exception is consistent with the thicker sea ice in CESM2-lessmelt being more resilient to ice cover changes but more sensitive to ice volume changes due to a weaker thickness-ice growth feedback. The second time period when there are trend differences occurs in the 2060s and 2070s. This exception occurs because CESM2-lessmelt still has ice to lose while CESM2-LE is ice-free already in September (**Figure 11c**). As a result, CESM2-lessmelt has more negative September sea ice extent trends than CESM2-LE during the 2060s and 2070s. Similar trend differences associated with timing differences to an ice-free Arctic are seen in October and August, but shifted later in the 21st century (not shown). The last time period is for trend end dates around 1970 when the volume trends in CESM2-lessmelt are larger than those in CESM2-LE.

We finish comparing the 1850-2100 transient sea ice evolution by contrasting interannual sea ice variability in CESM2-lessmelt and CESM2. As was done for means, we bootstrap the CESM2-LE to create variability estimates consistent with an ensemble with only 4 members. Consistent with previous work (Goosse et al. 2009, Mioduszewski et al. 2019), we find Arctic sea ice cover variability strongly depends on the mean sea ice thickness in CESM2 and CESM2-lessmelt (**Figure S9**). Overall, September sea ice extent interannual variability is smaller in CESM2-lessmelt than in CESM2 until the middle of the 21st century. Smaller September sea ice variability in CESM2-lessmelt is especially seen during the turn of the century forced sea ice decline (20 year trends ending ~2010). After the 2040s, CESM2-lessmelt has more year-to-year September sea ice extent variability than CESM2 because CESM2-lessmelt transitions to a seasonally ice-free Arctic later than CESM2.

3.4. Influence of sea ice mean state on transient climate change

We next assess the impact of the differing CESM2 and CESM2-lessmelt 1850-2100 sea ice evolution on transient climate change more broadly. In the end, we focus on surface warming for two reasons. First, climate impacts often scale with surface warming. As a result, assessing where/when warming differences occur provides a foundation for assessing if the CESM2 and CESM2-lessmelt sea ice evolution differences impact climate change and variability more broadly. Second, we investigated other climate variables such as precipitation and sea level pressure and found that differences in the transient climate response in CESM2 and CESM2-lessmelt were small and not statistically significant (**e.g., Figure S10**). One exception was smaller

21st century winter Arctic precipitation increases in CESM2-lessmelt than in CESM2. This exception is consistent with Clausius–Clapeyron relation, namely a reduced water vapor increase associated with less warming in CESM2-lessmelt than in CESM2.

When plotted as anomalies, the 1850-2100 evolution of the global mean surface temperature anomaly in CESM2 and CESM2-lessmelt are indistinguishable (Figure 13a). Both CESM2 model variants are consistent with the observed global air surface temperature anomaly evolution (Hansen et al. 2010). When plotted as absolute values, the global mean surface temperature is lower in CESM2-lessmelt than CESM2 (**Figure 13b**). This absolute temperature difference between the two CESM2 variants remains constant over the entire 1850-2100 period. Moreover, the spatial pattern of seasonal warming in CESM2-lessmelt and CESM2 is statistically indistinguishable aside from two notable exceptions in the Arctic (**Figure 14**). First, CESM2-lessmelt warms more than CESM2 along the sea ice edge during Fall, particularly in the Pacific sector. This larger warming occurs because CESM2-lessmelt has more sea ice to lose in these regions than CESM2 (**Figure 2b**). Second, CESM2 warms more than CESM-lessmelt in the central Arctic Ocean during winter. This difference arises because CESM2 has thinner sea ice than CESM2-lessmelt.

While the total zonal mean warming over the period 1920-1939 to 2080-2099 is remarkably similar in CESM2 and CESM2-lessmelt, when that warming happens differs between the two model variants in the Arctic. Indeed, comparisons of zonal mean warming rates in CESM2 and CESM2-lessmelt show differences in the Arctic warming rates in all seasons except summer (**Figure 15**). In particular, CESM2 has large non-summer surface Arctic warming rates earlier than CESM2-lessmelt. These larger early warming rates in CESM2 results from an earlier transition towards an ice-free Arctic Ocean in CESM2 than in CESM2-lessmelt.

4. Summary and Discussion

This study assesses the influence of sea ice mean state on simulated climate change and variability in a state-of-the-art global coupled climate model. Novel and new here, a large 50-member large ensemble is leveraged as a control for assessing the new small 4-member ensemble with more mean state sea ice, especially in the Arctic. As large initial condition ensembles are generally run after model releases, we address a question that is unanswerable during model development: *Do differences in the pre-industrial control sea ice mean state alter the ensemble spread of realized transient climate change?* Our results re-enforce that a realistic Arctic mean state is critical to simulating a realistic transition to an ice-free Arctic Ocean. Specifically, simulations with the same global warming but more Arctic sea ice in their pre-industrial control have a later transition to a late summer ice-free Arctic over the 21st century. These results demonstrate starting with a reasonable initial state is important for trusting model-projected timing towards an ice-free Arctic Ocean in a warming world. Important for climate projections and model development more generally, the sea ice differences examined here had negligible impacts outside the polar regions.

Interestingly, many commonly used metrics to benchmark sea ice simulations provide limited value in this study. While ensemble means best emphasize differences between model versions, ensemble mean values are not physically realized quantities, mute internal variability, and thus were not compared as equals with observed timeseries and trends (Kay et al. 2015, Deser et al. 2012). Assuming any individual ensemble member is equally likely, many metrics struggle to differentiate between the thicker (CESM2-lessmelt) and thinner (CESM2) sea ice model variants examined here. For example, this study reinforces previous work showing a two decade uncertainty in the timing of an ice-free Arctic due to internally generated variability (Jahn et al. 2016, Notz 2015). Here, we find an almost four decade uncertainty in the timing of an ice-free Arctic in the first 50 members of the CESM2-LE due to the confluence of CMIP6 biomass burning forcing and thin CESM2 Arctic sea ice. In addition, sea ice sensitivity exhibits large spread in the first 50 CESM2-LE members and thus provides limited value as an observational constraint or a robust model comparison metric to CESM2-lessmelt. Finally, linear sea ice area trends were similar between CESM2 and CESM2-lessmelt ensemble members. The fact that such commonly used metrics provide limited differentiation in this study is sobering and merits emphasis. Internal variability is large and must be measured and accounted for when comparing model ensemble size, as was done here. Of course, these findings are not entirely surprising given similar global warming in CESM2 and CESM2-lessmelt. In other words, global warming cannot be used as constraint on simulated sea ice trends or sensitivity in this study. In fact, the mean state differences probed here were not large enough to cause Arctic sea ice trend differences for the same amount of global warming. As a result, this work does not refute previous work showing that global warming (e.g., Mahlstein and Knutti 2012, Roach et al. 2020) can constrain sea ice change, and can help illustrate when models have the right Arctic sea ice trends for the wrong reasons (e.g., Rosenblum and Eisenman 2017). In summary, the similarity between CESM2 and CESM2-tuned found here provides further evidence that global warming exerts strong controls on Arctic sea ice trends.

We end by discussing lessons learned for simulation of sea ice in a global coupled climate modeling framework. We began this study by reducing sea ice surface melt in a pre-industrial control simulation in search of a stable model configuration with more Arctic Ocean sea ice volume and late summer Arctic Ocean sea ice cover. The parameter modifications implemented in CESM2-lessmelt were specifically targeted to reduce summer melt in the Arctic where surface melt dominates. Unlike the Arctic, Antarctic sea ice melt is dominated by bottom melt. Thus, we anticipated and found relatively small differences in the Antarctic sea ice mean state as a result of our parameter modifications. After obtaining a stable multi-century control run, we then ran transient 1850-2100 simulations with no additional changes. What emerged in the transient simulations was influenced both by the mean state and by feedbacks in CESM2, and was a surprise to us. Indeed, our success in obtaining more realistic transition to an ice-free Arctic state with CESM2-tuned suggests that sea ice thickness and late summer cover are important targets for sea ice in coupled model development. In contrast, attention to and tuning of Arctic sea ice area alone is generally insufficient. That said, sea ice area expansion is important to monitor and model development should focus on parameters and physics that lead to credible sea ice area distributions. The North Atlantic is especially important to monitor as when sea ice expands to completely cover the ocean there, it can shut down North Atlantic deep water formation, and derail global coupled earth system model development as discussed in Danabasoglu et al. (2021).

Acknowledgments and Data

J.E.K. was supported by National Science Foundation (NSF) CAREER 1554659. P. D. was supported by the Natural Sciences and Engineering Council of Canada (NSERC), the Fond de recherche du Québec – Nature et Technologies (FRQNT) and the Canadian Meteorological and Oceanographic Society (CMOS) through Ph.D. scholarships and by NSF CAREER 1554659, and NSF CAREER 1847398. M.M.H., D.A.B., A.D., C.D., J.E., and N.R. acknowledge support by the National Center for Atmospheric Research (NCAR), which is a major facility sponsored by the NSF under Cooperative Agreement 1852977. M. M. H. was additionally supported by NSF-OPP 1724748. A.J. was supported by NSF CAREER 1847398. M.M.S. was supported by NSF OPP-1724467 and OPP-172474. M.A.W. was provided by NASA's New (Early Career) Investigator Program in Earth Science Award 80NSSC20K0658. S.-S..L. and K.B.R.. were supported by IBS-R028-D1. The CESM project and NCAR are supported primarily by NSF. Computing and data storage resources for developing CESM2, CESM2-lessmelt, and CESM2-LE were provided by the Computational and Information Systems Laboratory (CISL) at NCAR, including the Cheyenne supercomputer (doi:10.5065/D6RX99HX). The CESM2-LE simulations were run on the IBS/ICCP supercomputer "Aleph", a 1.43 petaflop high-performance Cray XC50-LE Skylake computing system with 18,20 processor cores, with 9.59 petabytes of disc storage, and 43 petabytes of tape archive storage. CESM2-LE data are available here: https://www.cesm.ucar.edu/projects/community-projects/LENS2/. The CESM2-lessmelt data are available via Globus access to NCAR GLADE at: /glade/campaign/cgd/ppc/cesm2_tuned_albedo. For more information on using Globus on NCAR systems, please refer to https://www2.cisl.ucar.edu/resources/storage-and-file-systems/globus-file-transfers

References

Bailey, D. A., Holland, M. M., DuVivier, A. K., Hunke, E. C., & Turner, A. K. (2020). Impact of a new sea ice thermodynamic formulation in the CESM2 sea ice component. *Journal Of Advances In Modeling Earth Systems*, 12, e2020MS002154. doi:10.1029/2020MS002154

Bitz, C. M, Holland, M. M., Hunke, E. & Moritz, R. E. (2005). Maintenance of the sea-ice edge, *J. Climate*, 18, 2903-2921.

Bitz, C. M. (2008). Some aspects of uncertainty in predicting sea ice thinning, in Arctic Sea Ice Decline: observations, projections, mechanisms, and implications, AGU Geophysical Monograph Series, vol, edited by E. deWeaver, C. M. Bitz, and B. Tremblay, pp. 63-76 , American Geophysical Union.

Bitz, C. M. & Roe, G. H. (2004). A Mechanism for the High Rate of Sea-Ice Thinning in the Arctic Ocean, *J. Climate*, 17, 3622--31

Blanchard-Wrigglesworth E., Bitz, C.M. & Holland, M.M. (2011). Influence of initial conditions and climate forcing on predicting Arctic sea ice, *Geophysical Research Letters*, 38, L18503, doi: 10.1029/2011GL048807

Bonan, D. B., Lehner, F. & Holland, M. (2021). Partitioning uncertainty in projections of Arctic sea ice, *Environmental Research Letters*, DOI: 10.1088/1748-9326/abe0ec

Briegleb, B. P., & Light, B. (2007). A delta-Eddington multiple scattering parameterization for solar radiation in the sea ice component of the Community Climate System Model. NCAR Tech. Note TN-4721STR, 100 pp.

Danabasoglu, G., Lamarque, J.-F., Bachmeister, J., Bailey, D. A., DuVivier, A. K., Edwards, J., Emmons, L. K., Fasullo, J., Garcia, R., Gettelman, A., Hannay, C., Holland, M. M., Large, W. G., Lawrence, D. M., Lenaerts, J. T. M., Lindsay, K., Lipscomb, W. H., Mills, M. J., Neale, R., Oleson, K. W., Otto-Bliesner, B., Phillips, A. S., Sacks, W., Tilmes, S., van Kampenhout, L., Vertenstein, M., Bertini, A., Dennis, J., Deser, C., Fischer, C., Fox-Kemper, B., Kay, J. E., Kinnison, D., Kushner, P. J., Long, M. C., Mickelson, S., Moore, J. K., Nienhouse, E., Polvani, L., Rasch, P. J., & Strand, W. G. (2020). The Community Earth System Model version 2 (CESM2). Journal of Advances in Modeling Earth Systems, 12, e2019MS001916. https://doi.org/10.1029/2019MS001916

DeRepentigny, P., Jahn., A., Holland, M. M., Fasullo, J., Lamarque, J.-F., Hannay, C., Mills, M. J., Bailey, D. Tilmes, S., & Barrett, A. (2021). Enhanced early 21st century Arctic sea ice loss due to CMIP6 biomass burning emissions, *Nature Climate Change*, under review, Available here: https://bit.ly/3Ahkjj1

DeRepentigny, P., Jahn, A., Holland, M. M., & Smith, A. (2020). Arctic sea ice in the two

Community Earth System Model Version 2 (CESM2) configurations during the 20th and 21st centuries. Journal of Geophysical Research: Oceans, 125, e2020JC016133. https://doi.org/10.1029/2020JC016133

Deser, C., Lehner, F., Rodgers, K.B. et al. (2020). Insights from Earth system model initial-condition large ensembles and future prospects. *Nat. Clim. Chang.* 10, 277–286, https://doi.org/10.1038/s41558-020-0731-2

Deser, C., R. Knutti, , S. Solomon, & Phillips, A. S. (2012). Communication of the role of natural variability in future North American climate. *Nat. Climate Change*, 2, 775–779, doi:10.1038/nclimate1562.

Deser, C., R. Tomas, M. Alexander, & Lawrence, D. (2010). The seasonal atmospheric response to projected Arctic sea ice loss in the late 21st century. *J. Climate*, 23, 333-351, 10.1175/2009JCLI3053.1.

DuVivier, A., Holland, M., Kay, J. E., S. Tilmes, A. Gettelman, & Bailey, D. (2020), Arctic and Antarctic sea ice state in the Community Earth System Model Version 2, *Journal of Geophysical Research—Oceans*, http://dx.doi.org/10.1029/2019JC015934

Eyring, V., Bony, S., Meehl, G. A., Senior, C. A., Stevens, B., Stouffer, R. J., & Taylor, K. E. (2016). Overview of the Coupled Model Intercomparison Project Phase 6 (CMIP6) experimental design and organization, *Geosci. Model Dev.*, 9, 1937–1958, https://doi.org/10.5194/gmd-9-1937-2016.

Fasullo, J. T., Lamarque, J-F, Hannay, C., Rosenbloom, N., Tilmes, S., DeRepentigny, P., Jahn, A., & Deser, C. (2021). Spurious Late Historical-Era Warming in CESM2 and Other CMIP6 Climate Simulations Driven by Prescribed Biomass Burning Emissions, *Nature Climate Change*, under review, Available here: https://bit.ly/360yXNv

Fetterer, F., K. Knowles, W. N. Meier, M. Savoie, & Windnagel, A. K. (2017), Sea Ice Index, Version 3. [1979-2020]. Boulder, Colorado USA. NSIDC: National Snow and Ice Data Center. doi: https://doi.org/10.7265/N5K072F8.

Goosse, H., Arzel., O., Bitz, C. M., de Montety, A., & Vancoppenolle, M. (2009) Increased variability of the Arctic summer ice extent in a warmer climate, *Geophys. Res. Lett.*, 36, L23702, https://doi.org/10.1029/2009GL040546, 2009

Hansen, J., et al. (2010). Global surface temperature change, *Rev. Geophys.*, 48, RG4004, doi:10.1029/2010RG000345

Holland, M.M., L. Landrum, D. Bailey, & Vavrus, S.J. (2019). Changing seasonal predictability of Arctic summer sea ice area in a warming climate. *J. Climate*, doi:10.1175/JCLI-D-19-0034.1

Holland, M.M., D.A. Bailey, & Vavrus, S. (2011). Inherent sea ice predictability in the rapidly changing Arctic environment of the Community Climate System Model, version 3, *Climate Dynamics*, 36, 1239-1253, doi:10.1007/s00382-010-0792-4.

Holland, M.M., & Stroeve, J. (2011). Changing seasonal sea ice predictor relationships in a changing Arctic climate. *Geophys. Res. Lett.*, 38, L18501, doi:10.1029/2011GL049303.

Holland, M. M., M. C. Serreze, & Stroeve, J. (2010). The sea ice mass budget of the Arctic and its future change as simulated by coupled climate models, *Climate Dynamics*, 34, 185–200, doi:10.1007/s00382-008-0493-4.

Holland, M.M., C.M. Bitz, & Tremblay, B. (2006). Future abrupt reductions in the Summer Arctic sea ice, *Geophys. Res. Lett.*, 33, L23503, doi:10.1029/2006GL028024.

Hunke E. C., W. H. Lipscomb, A. K. Turner, N. Jeffery, & Elliott, S. (2015). CICE: The Los Alamos Sea Ice Model. Documentation and Software User's Manual. Version 5.1. T-3 Fluid Dynamics Group, Los Alamos National Laboratory, Tech. Rep. LA-CC-06-012.

Jahn, A. (2018). Reduced probability of ice-free summers for 1.5 °C compared to 2 °C warming. *Nature Climate Change*, 8: 409-413. DOI: 10.1038/s41558-018-0127-8

Jahn, A., Kay, J. E., Holland, M. M., & Hall, D. M. (2016). How predictable is the timing of a summer ice-free Arctic?. *Geophysical Research Letters*, 43(17): 9113-9120. DOI: 10.1002/2016GL070067

Kay, J. E., Deser, C., Phillips, A., Mai, A., Hannay, C., Strand, G., Arblaster, J., Bates, S., Danabasoglu, G., Edwards, J., Holland, M. Kushner, P., Lamarque, J.-F., Lawrence, D., Lindsay, K., Middleton, A., Munoz, E., Neale, R., Oleson, K., Polvani, L., & Vertenstein, M. (2015). The Community Earth System Model (CESM) Large Ensemble Project: A Community Resource for Studying Climate Change in the Presence of Internal Climate Variability, *Bulletin of the American Meteorological Society*, 96, 1333–1349. doi:10.1175/BAMS-D-13-00255.1.

Kay, J. E., Holland, M. M., & Jahn, A. (2011). Inter-annual to multi-decadal Arctic sea ice extent trends in a warming world. *Geophysical Research Letters*, 38, L15708. https://doi.org/10.1029/2011GL048008

Kirchmeier-Young, M. C., F. W. Zwiers, & Gillett, N. P. (2017). Attribution of extreme events in Arctic sea ice extent, *J. Clim.*, 30, 553–571 doi:10.1175/JCLI-D-16-0412.1.

Latif, M., T. Martin, & Park, W. (2013). Southern Ocean sector centennial climate variability and recent decadal trends, *J. Clim.*, 26(19), 7767–7782.

Mahlstein, I., & Knutti, R. (2012). September Arctic sea ice predicted to disappear near 2°C global warming above present, *J. Geophys. Res.*, 117, D06104, doi:10.1029/2011JD016709.

Massonnet, F., Vancoppenolle, M., Goosse, H., Docquier, D., Fichefet, T., & Blanchard-Wrigglesworth, E. (2018). Arctic sea-ice change tied to its mean state through thermodynamic processes. *Nature Climate Change*, 8(7), 599–603. https://doi.org/10.1038/s41558-018-0204-z

Mauritsen, T., Stevens, B., Roeckner, E., Crueger, T., Esch, M., Giorgetta, M., et al. (2012). Tuning the climate of a global model. *Journal of Advances in Modeling Earth Systems*, 4, M00A01. https://doi.org/10.1029/2012MS000154

Mioduszewski, J., S. Vavrus, M. Wang, M. Holland, & Landrum, L. (2019). Past and future interannual variability in Arctic sea ice in coupled climate model. *Cryosphere*, 13, 113–124, https://doi.org/10.5194/tc-13-113-2019.

Notz, D. (2015). How well must climate models agree with observations? *Philosophical Transactions of the Royal Society A*, 373(2052), 20140164. https://doi.org/10.1098/rsta.2014.0164

O'Neill, B. C., Tebaldi, C., van Vuuren, D. P., Eyring, V., Friedlingstein, P., Hurtt, G., Knutti, R., Kriegler, E., Lamarque, J.-F., Lowe, J., Meehl, G. A., Moss, R., Riahi, K., and Sanderson, B. M. (2016). The Scenario Model Intercomparison Project (ScenarioMIP) for CMIP6, *Geosci. Model Dev.*, 9, 3461–3482, https://doi.org/10.5194/gmd-9-3461-2016.

Phillips, A. S., C. Deser, J Fasullo, D. P. Schneider & Simpson, I. R. (2020). Assessing Climate Variability and Change in Model Large Ensembles: A User's Guide to the "Climate Variability Diagnostics Package for Large Ensembles", doi:10.5065/h7c7-f961

Roach, L. A., Dörr, J., Holmes, C. R., Massonnet, F., Blockley, E. W., Notz, D., & Bitz, C. M. (2020). Antarctic sea ice in CMIP6. *Geophysical Research Letters*, 47, e2019GL086729. https://doi.org/10.1029/2019GL086729

Rodgers, K., Lee, S-S., Rosenbloom, N., Timmerman, A., Danabasoglu, G., Deser, C.., Edwards, J., Kim, J-E., Simpson, I., Stein, K, Stuecker, M., F., Yamaguchi, R., Bodai, T., Chang, E-S., Huang, L., Kim, W. M., Lamarque, J.-F., Lombardozzi, D., Wieder, W. R., and S. G. Yeager (2021), Ubiquity of human-induced changes in climate variability, submitted to *Earth System Dynamics*, https://doi.org/10.31223/X5GP79, Preprint available here: https://eartharxiv.org/repository/view/2444/

Rosenblum, E. & Eisenman, I. (2017). Sea ice trends in climate models only accurate in runs with biased global warming. *Journal of Climate*, 30(16), pp.6265-6278.

Sigmond, M., Fyfe, J. C. & N. C. Swart (2018). Ice-free Arctic projections under the Paris Agreement, *Nat. Clim. Change*, https://doi.org/10.1038/s41558-018-

0124-y (2018)

SIMIP Community (2020). Arctic Sea Ice in CMIP6, *Geophysical Research Letters*, 47(10): https://doi.org/10.1029/2019GL086749

Singh, H. K. A., Landrum, L., Holland, M. M., Bailey, D. A., & DuVivier, A. K. (2021). An overview of Antarctic sea ice in the Community Earth System Model version 2, part I: Analysis of the seasonal cycle in the context of sea ice thermodynamics and coupled atmosphere-ocean-ice processes. *Journal Of Advances In Modeling Earth Systems*, 13, e2020MS002143. doi:10.1029/2020MS002143

Swart, N. C., Fyfe, J. C., Hawkins, E., Kay, J. E., & Jahn, A. (2015), Influence of internal variability on Arctic sea-ice trends, *Nature Climate Change*, 5, 86-89, doi:10.1038/nclimate2483.

Taylor, K. E., R. J. Stouffer, & Meehl, G. A. (2012). The CMIP5 experiment design, *Bull. Am. Meteorol. Soc.*, 93, 485–498, doi:10.1175/BAMS-D-11-00094.1.

Webster, M. A., DuVivier, A. K., Holland, M. M., & Bailey, D. A. (2021). Snow on Arctic sea ice in a warming climate as simulated in CESM. *Journal Of Geophysical Research: Oceans*, 126, e2020JC016308. doi:10.1029/2020JC016308

Wettstein, J. J. & Deser, C. (2014). Internal variability in projections of twenty-first century Arctic sea ice loss: Role of the large-scale atmospheric circulation. *J. Climate*, 27, 527-550, doi: 10.1175/JCLI-D-12-00839.1.

Yeager, S., Karspeck, A., & Danabasoglu, G. (2015). Predicted slowdown in the rate of Atlantic sea ice loss. *Geophysical Research Letters*, 42, 10704-10713. doi:10.1002/2015GL065364

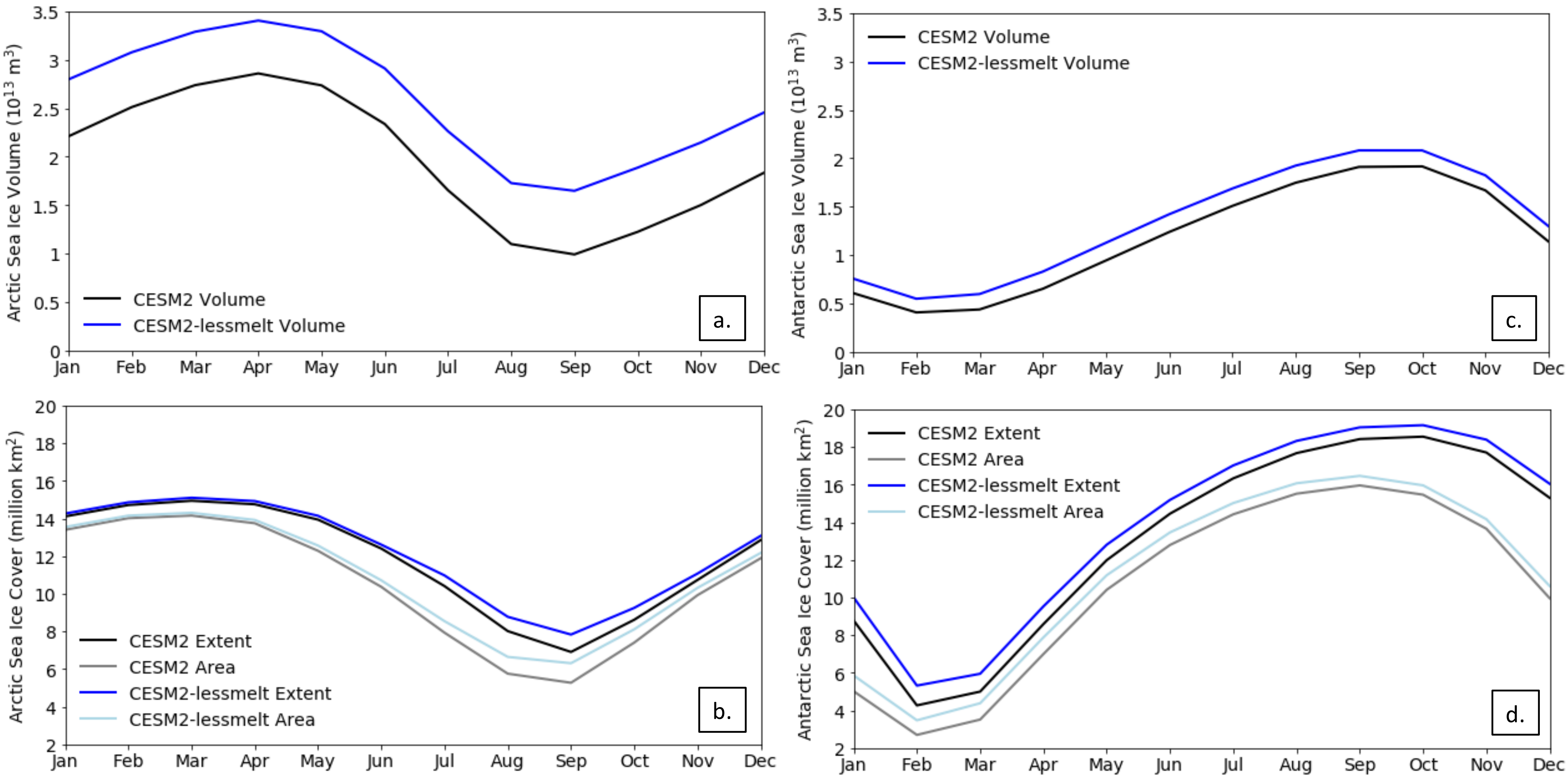

Figure 1. Seasonal cycle in CESM2 and CESM2-lessmelt 1850 preindustrial control runs: a) Arctic sea ice volume, b) Arctic sea ice area and extent, c) Antarctic sea ice volume, d) Antarctic sea ice area and extent. Values are overlapping 200-year averages (years 911-1110 of the CESM2 CMIP6 1850 pre-industrial control run).

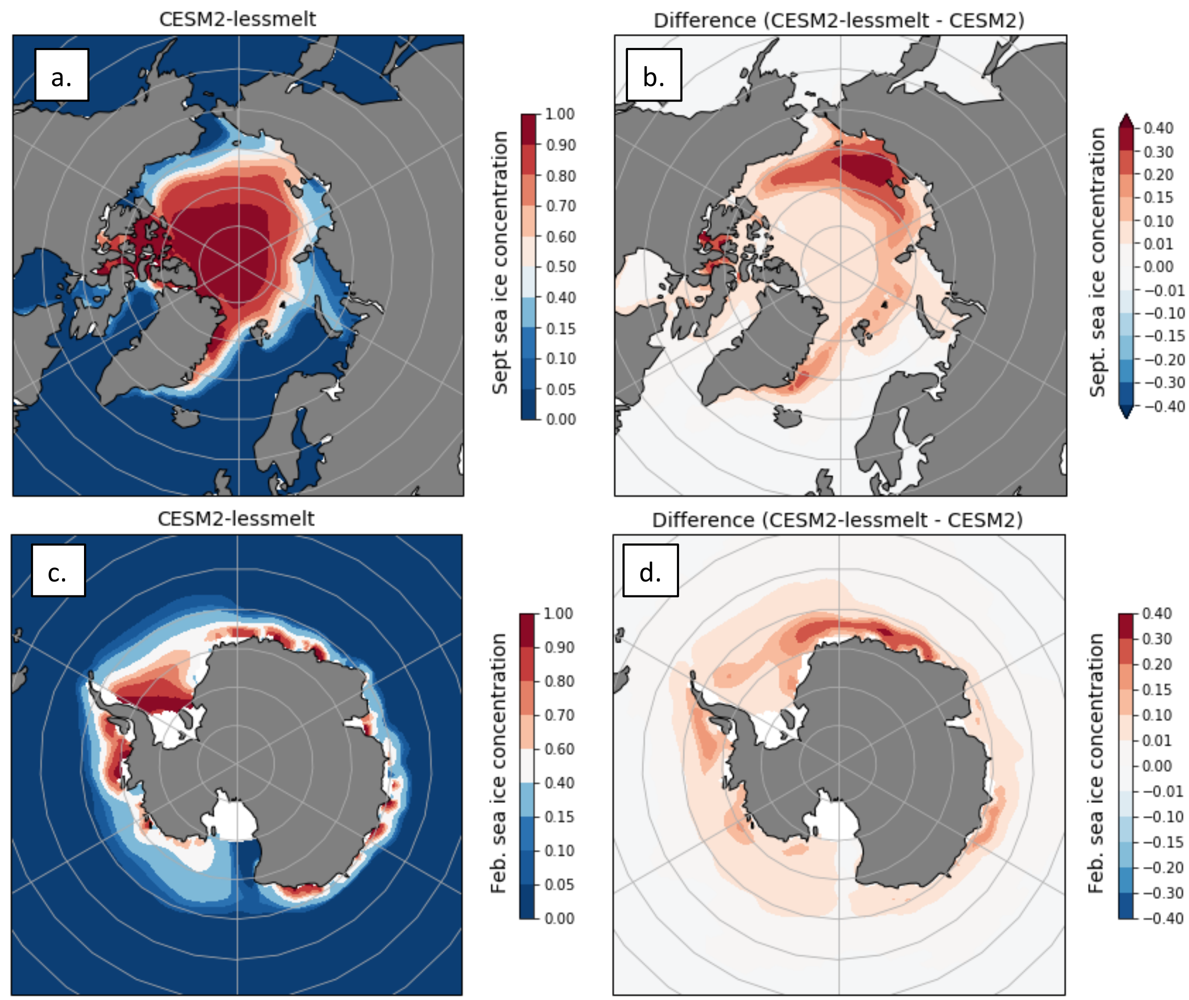

Figure 2. Late summer sea ice concentration in preindustrial control runs: a) September Arctic CESM2-lessmelt, b) Difference September Arctic (CESM2-lessmelt - CESM2), c) February Antarctic CESM2-lessmelt, d) Difference February Antarctic (CESM2-lessmelt - CESM2). Values are overlapping 200-year averages as in Figure 1. *Note: Nonlinear color scale used to emphasize thin ice categories.*

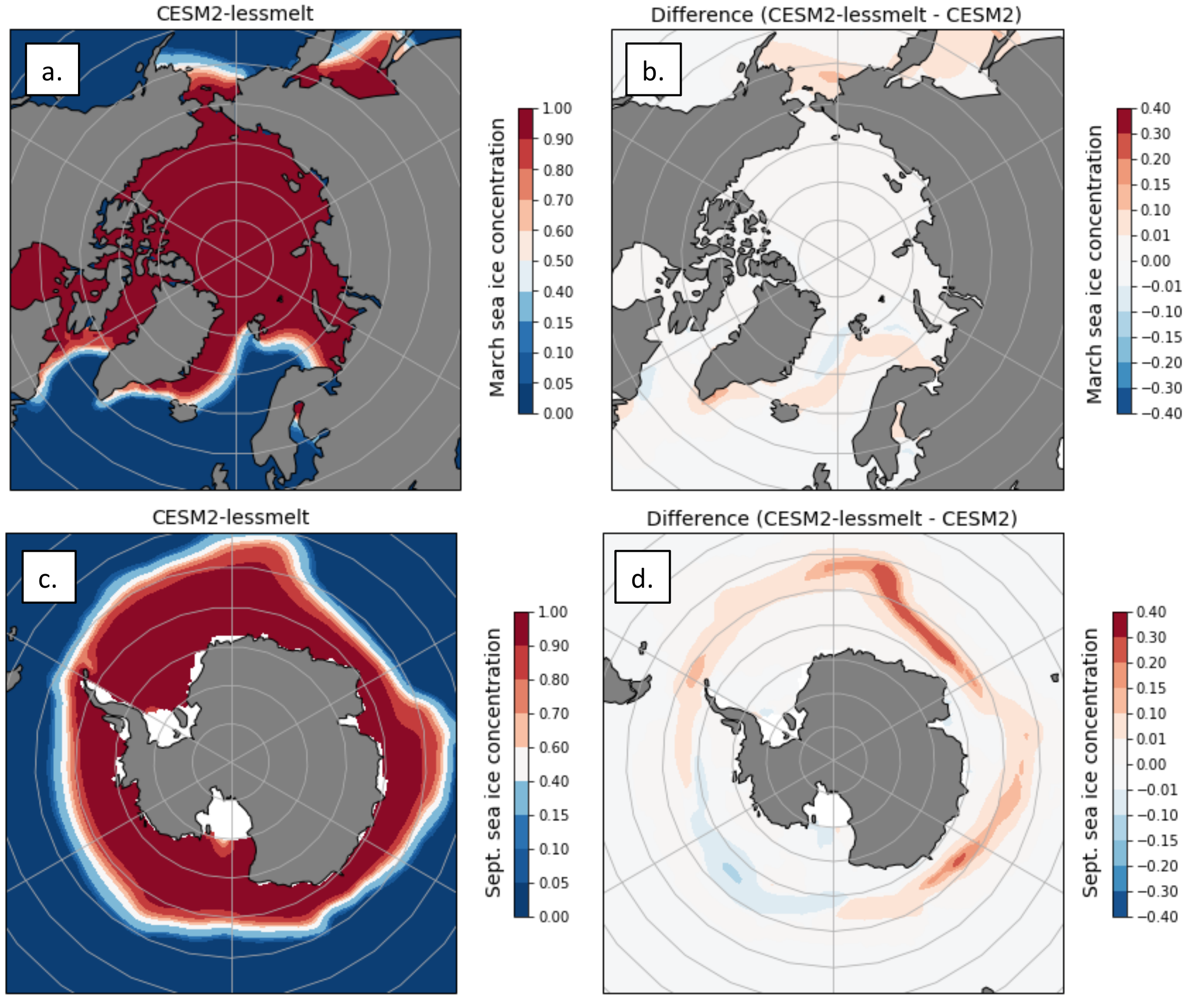

Figure 3. Late winter sea ice concentration in preindustrial control runs: a) CESM2-tuned ice March Arctic, b) Difference March Arctic, c) CESM2-lessmelt September Antarctic, d) Difference September Antarctic. Values are overlapping 200-year averages as in Figure 1. *Note: Nonlinear color scale used to emphasize thin ice categories.*

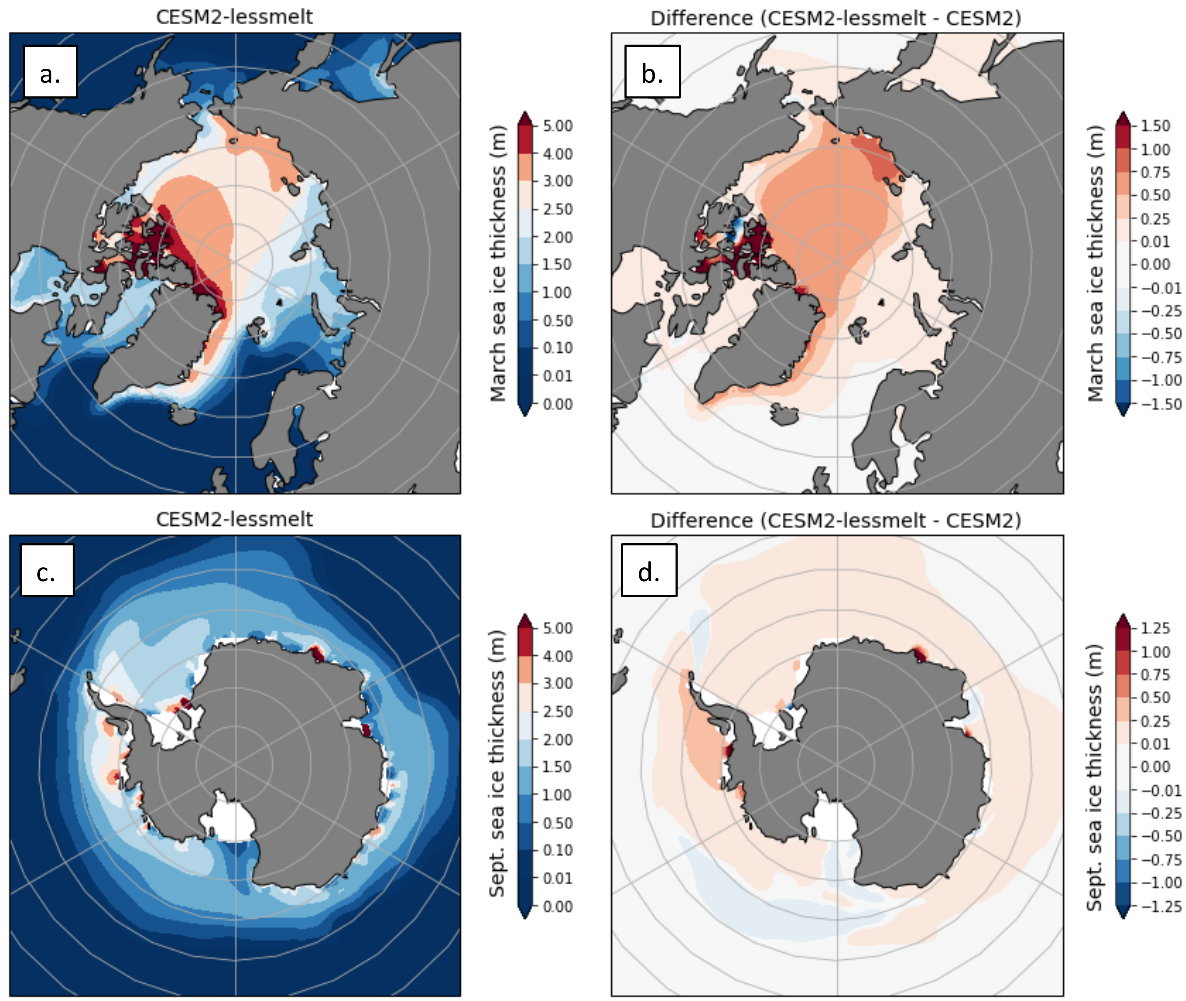

Figure 4. Late winter sea ice thickness in preindustrial control runs: a) CESM2 March Arctic, b) CESM2-lessmelt March Arctic, c) CESM2 September Antarctic, d) CESM2-lessmelt September Antarctic. Values are overlapping 200-year averages as in Figure 1. *Note: Nonlinear color scale used to emphasize thin ice categories.*

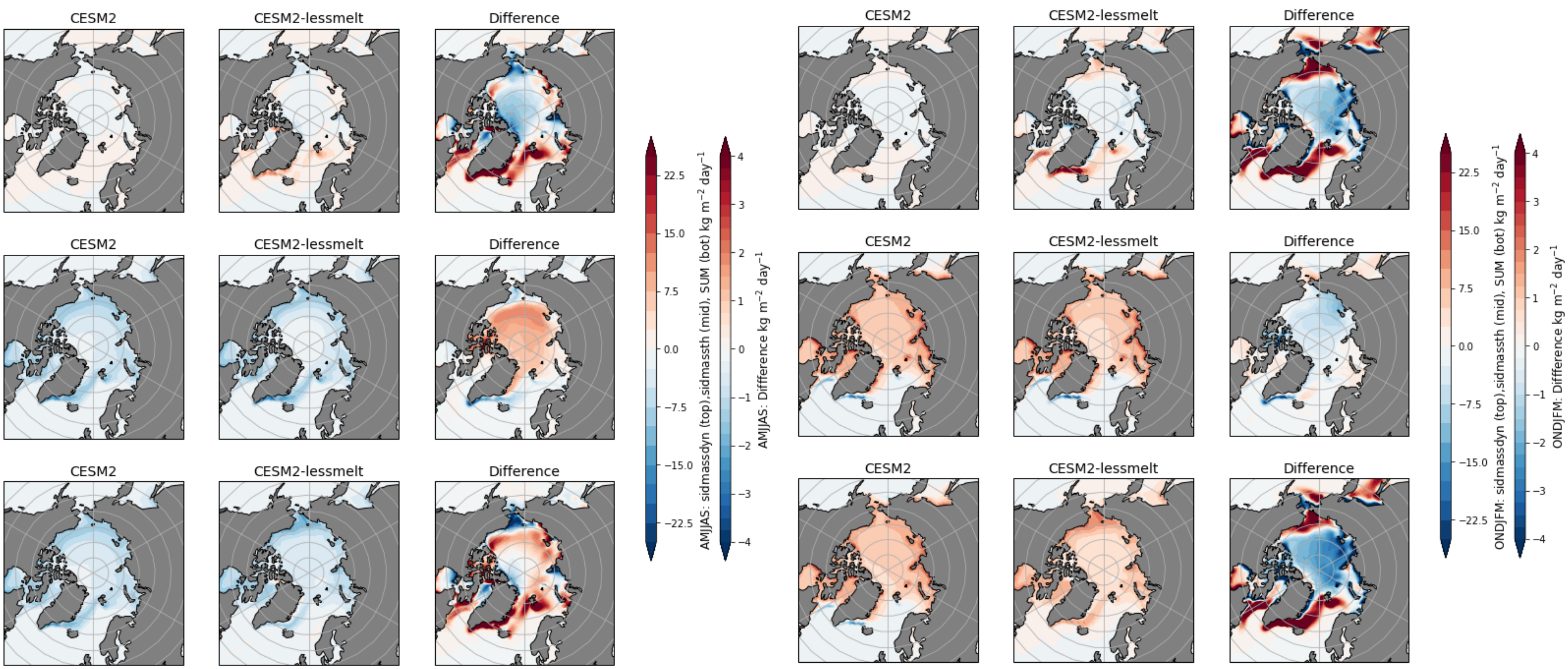

Figure 5. Arctic sea ice mass tendency terms for the melt season [AMJJAS] (left), and the growth season [ONDJFM] (right). For each season, the top row is tendency due to dynamics (sidmassdyn), the middle row is tendency due to thermodynamics (sidmassth), and the bottom row is their sum. All differences are CESM2-lessmelt minus CESM2. Values are overlapping 200-year averages as in Figure 1.

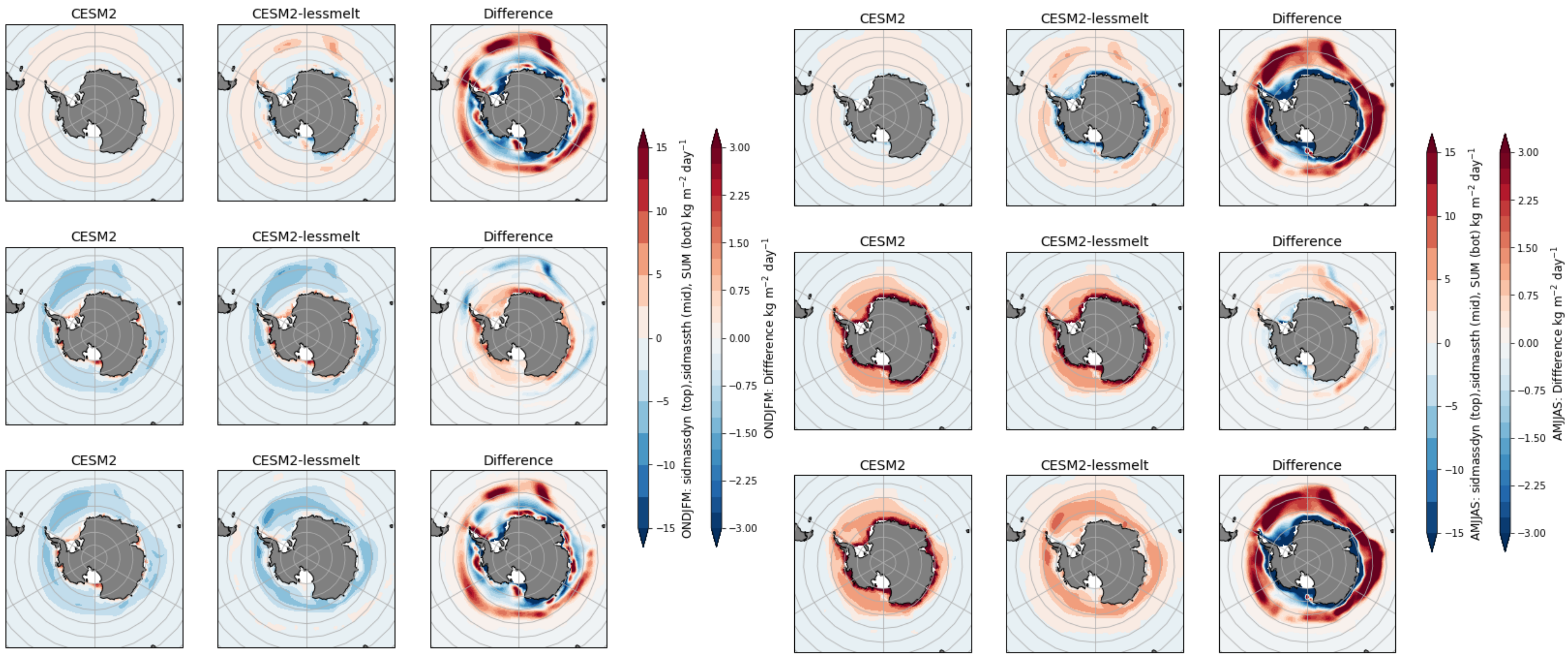

Figure 6. Antarctic sea ice mass tendency terms for the melt season [ONDJFM] (left), and the growth season [AMJJAS] (right). For each season, the top row is tendency due to dynamics (sidmassdyn), the middle row is tendency due to thermodynamics (sidmassth), and the bottom row is their sum. All differences are CESM2-lessmelt minus CESM2. Values are overlapping 200-year averages as in Figure 1.

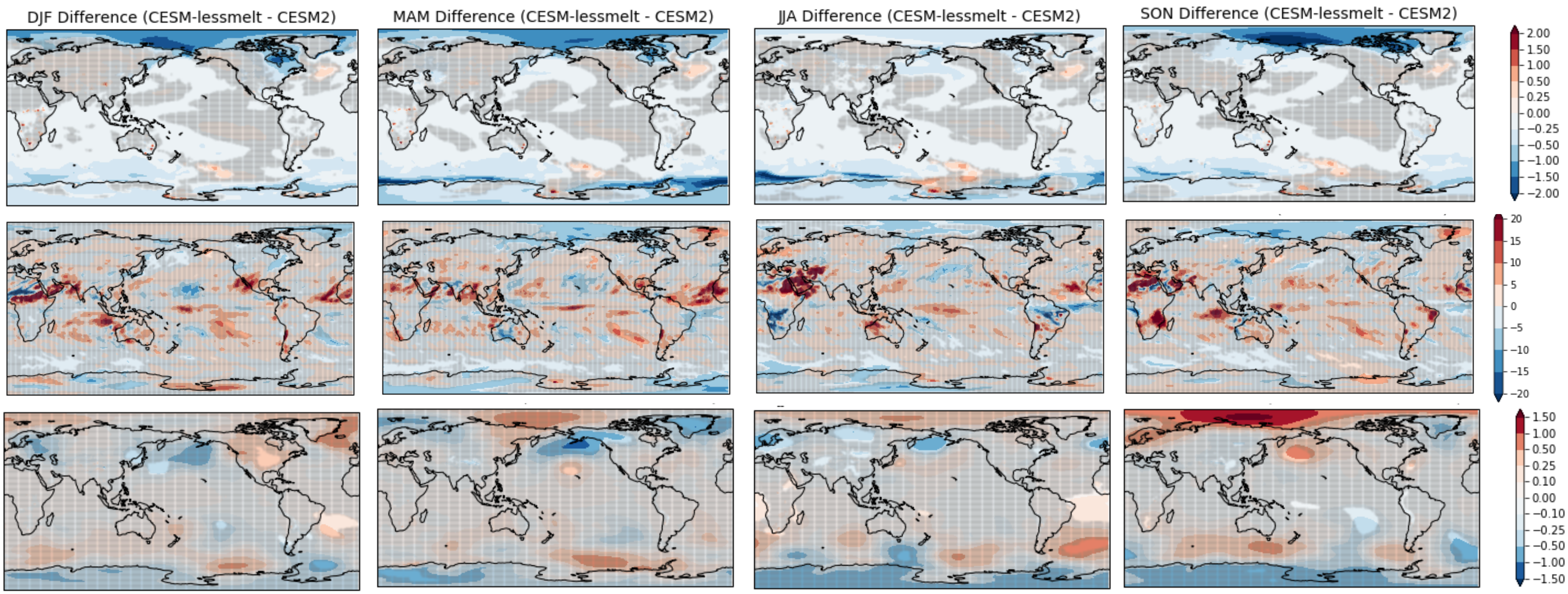

Figure 7. Global maps of difference in CESM2-lessmelt minus CESM2 pre-industrial by season. Top row shows surface temperature (K), Middle row shows total precipitation amount (% difference). Bottom row shows sea level pressure (mb). Grey stippling shows regions that are not statistically different at the 95% confidence level using a 2-sided t-test. Values are overlapping 200-year averages as in Figure 1.

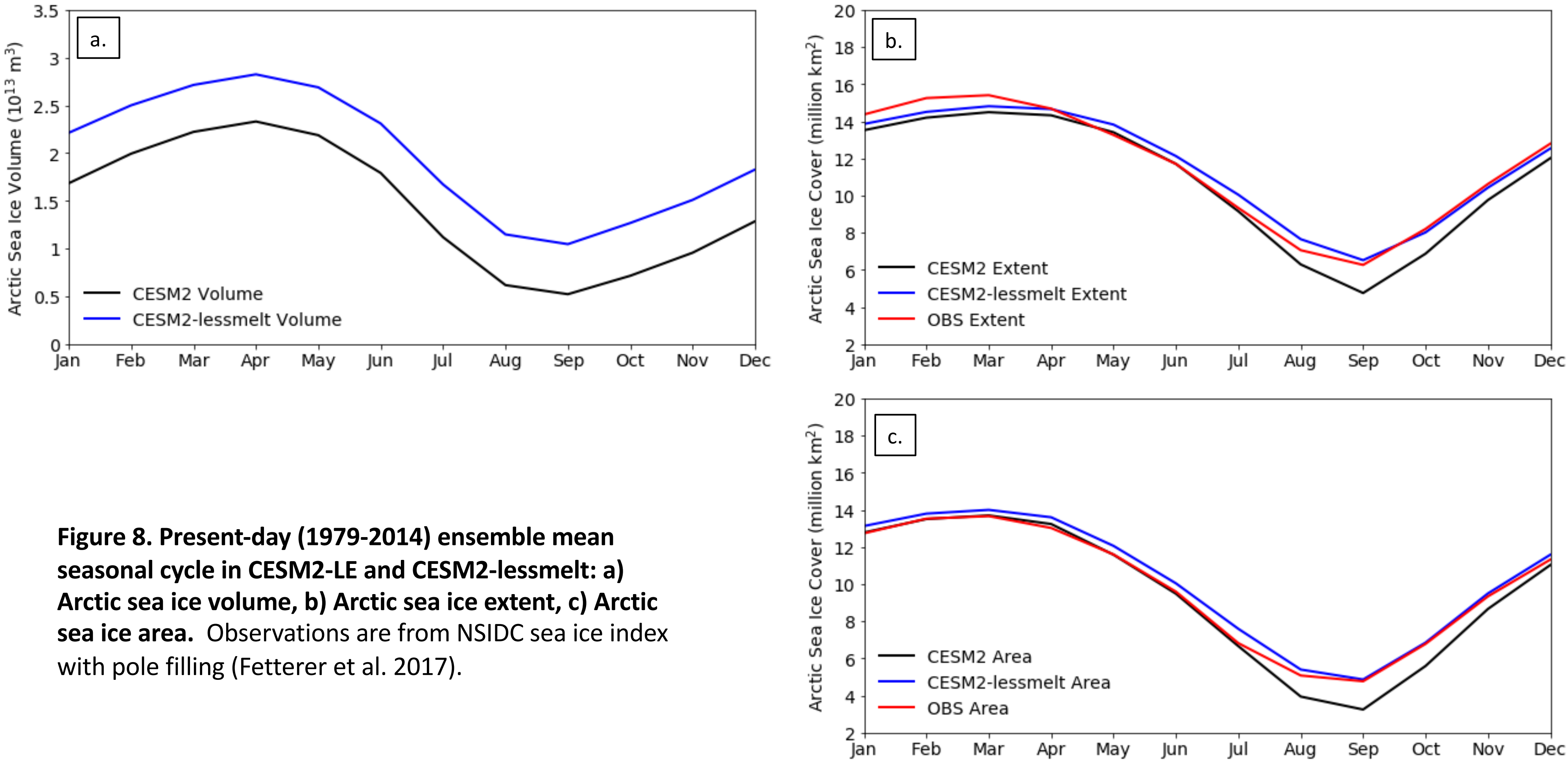

Figure 8. Present-day (1979-2014) ensemble mean seasonal cycle in CESM2-LE and CESM2-lessmelt: a) Arctic sea ice volume, b) Arctic sea ice extent, c) Arctic sea ice area. Observations are from NSIDC sea ice index with pole filling (Fetterer et al. 2017).

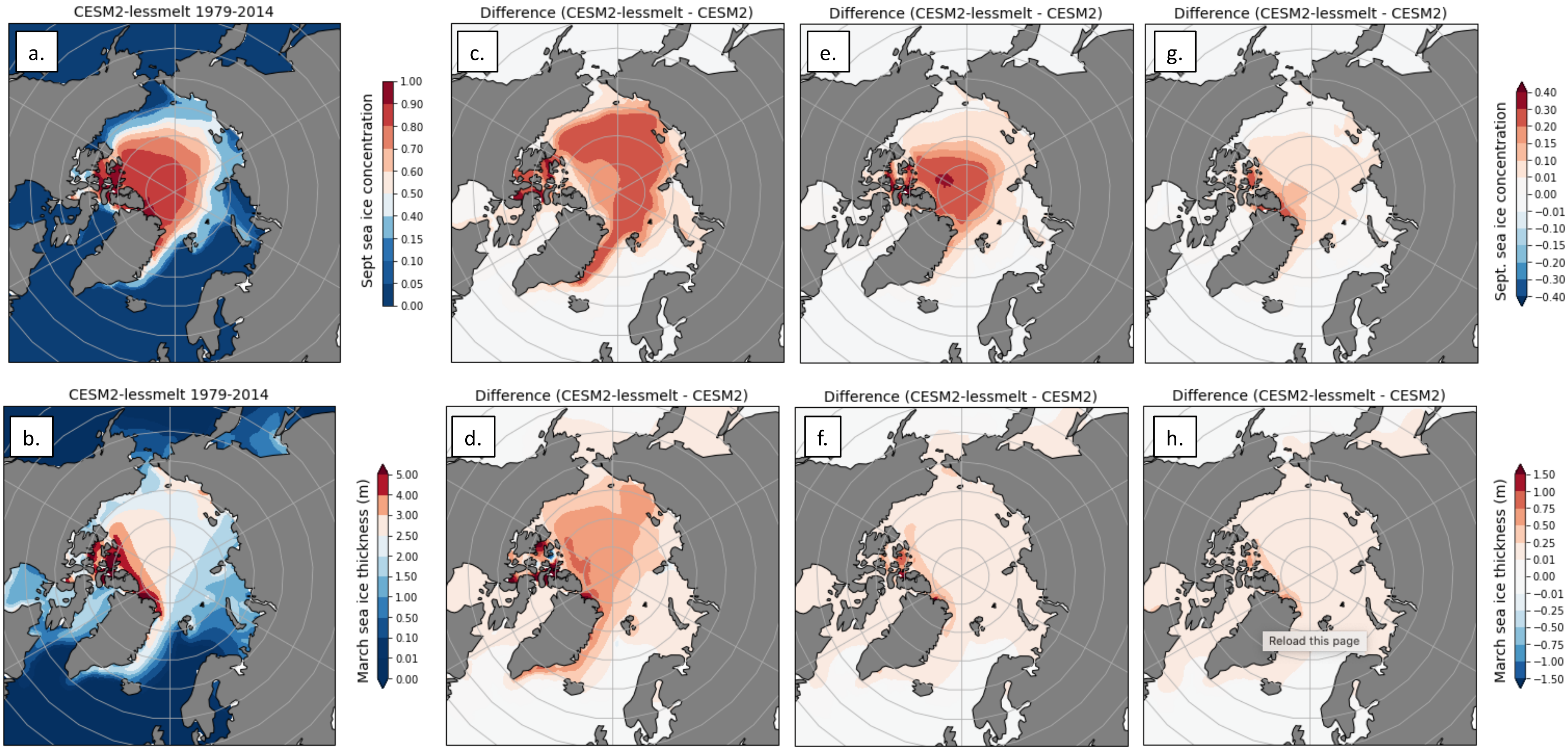

Figure 9. Ensemble mean Arctic sea ice maps: a) Present-day (1979-2014) CESM2-lessmelt September concentration, b) as in a) but for March thickness, c-d) as in a-b) but for the CESM2-lessmelt minus CESM2-LE difference, e-f) as in c-d) but for 2030-2049, g-h) as in c-d) but for 2050-2069

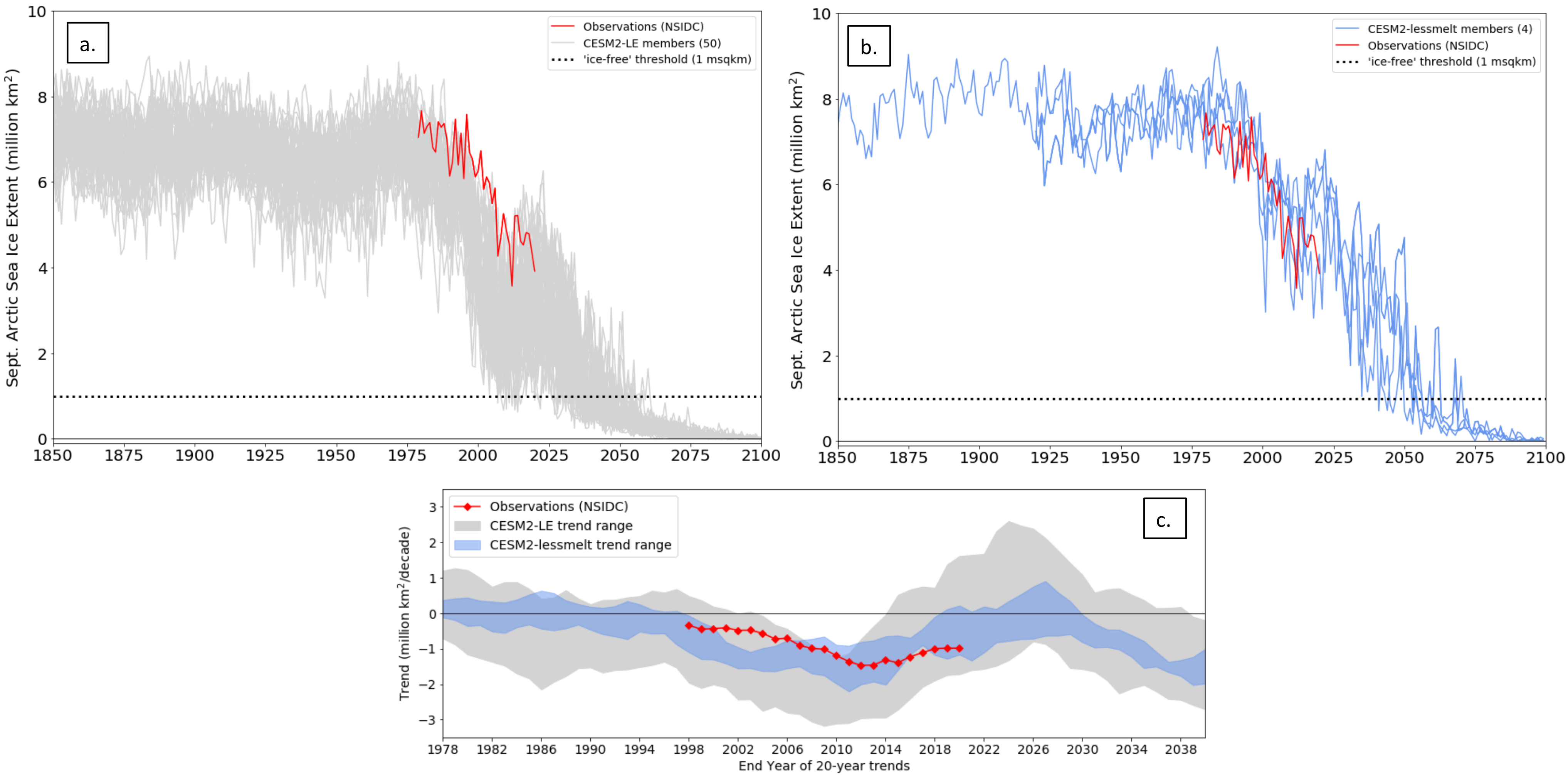

Figure 10. Arctic September sea ice extent transient evolution: a) CESM2-LE 1850-2100 timeseries, b) CESM2-lessmelt 1850-2100 timeseries, c) 20-year trends in CESM2-LE, CESM2-lessmelt, and observations with end years of 1999-2049. Observations are from NSIDC sea ice index (Fetterer et al. 2017) with area pole-filling.

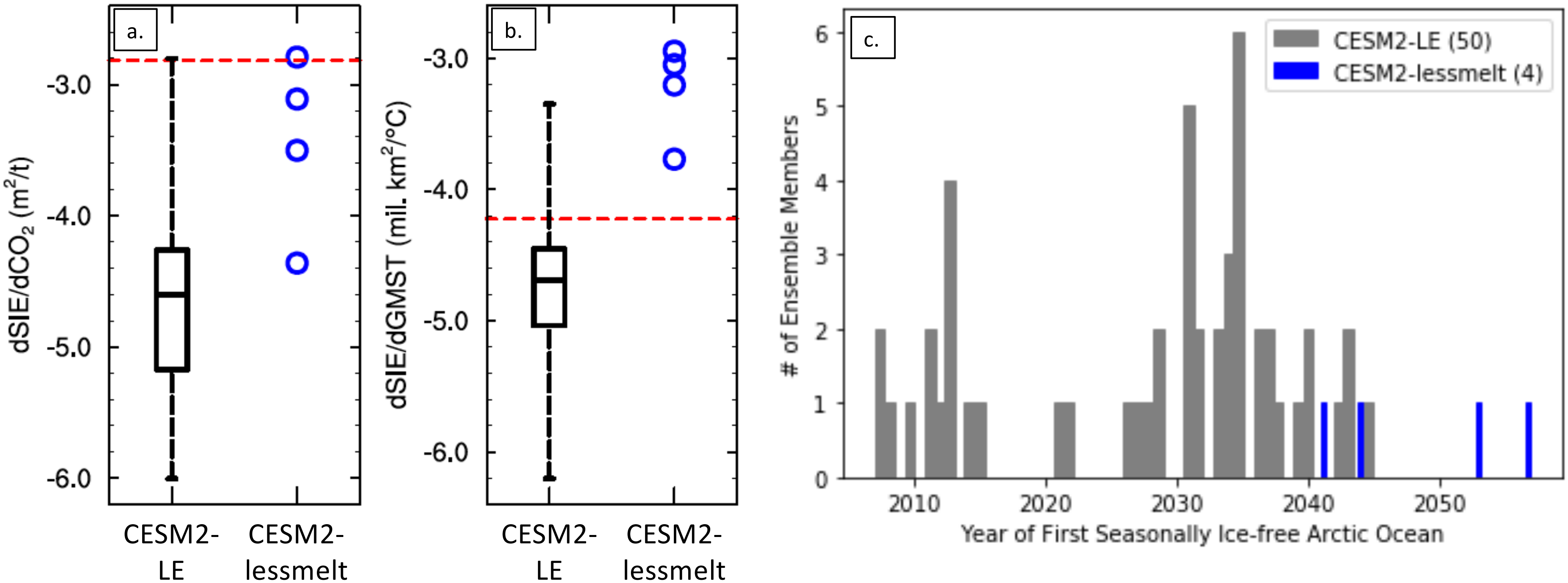

Figure 11. Arctic sea ice comparison metrics: a) Sea ice sensitivity defined as change in September sea ice extent per ton of cumulative atmospheric carbon dioxide emissions (dSIE/dCO_2), b) Sea ice sensitivity defined as change in September sea ice extent per degree global mean surface temperature (dSIE/dGMST), c) Year with first seasonally ice-free Arctic Ocean. Sea ice sensitivity calculations follow protocol and years (1979-2014) used for evaluation of CMIP6 models by the SIMIP Community (2020). Seasonally ice-free occurs when September sea ice extent first falls below 1 million sq. km.

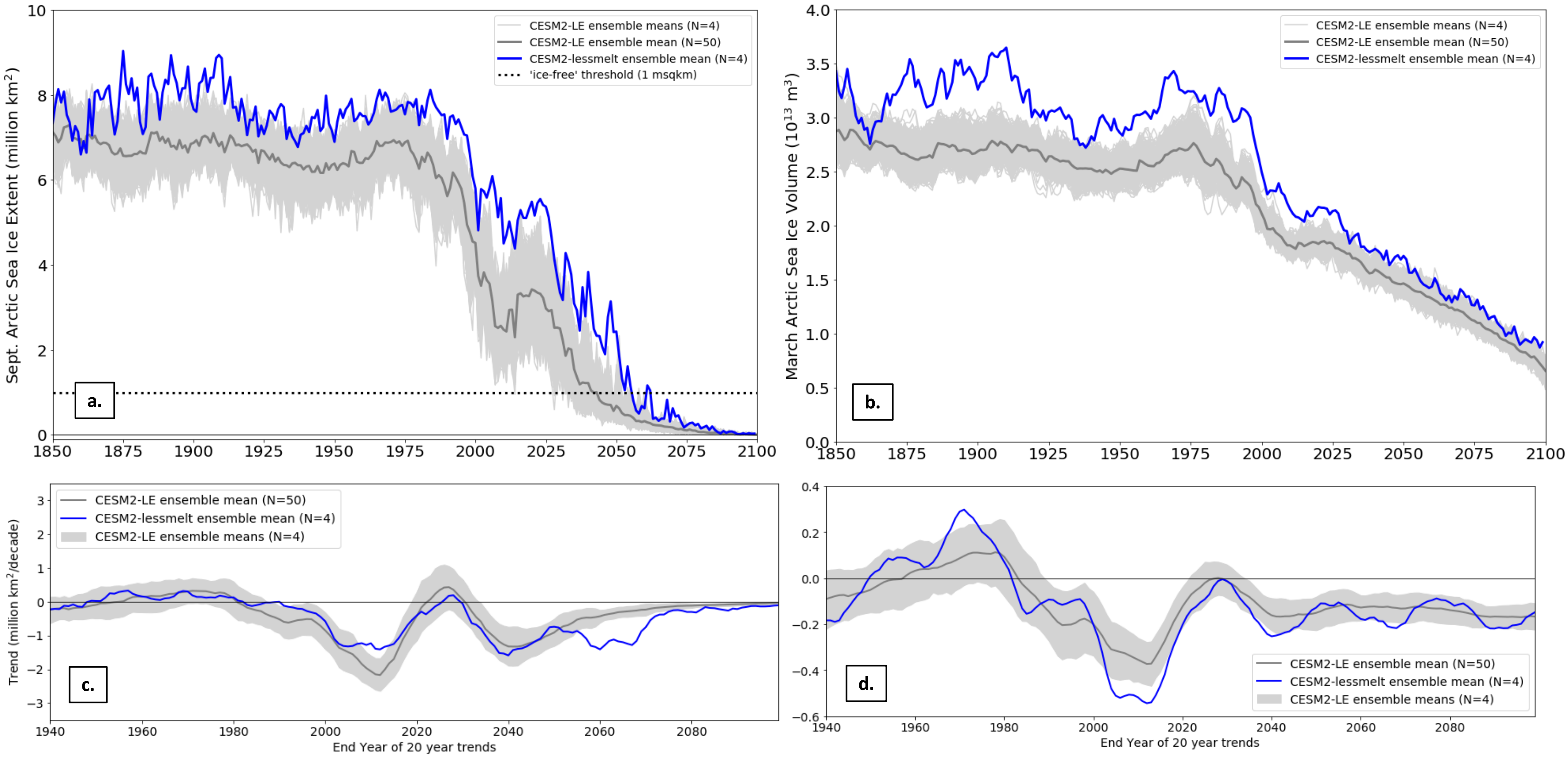

Figure 12. CESM2-LE and CESM2-lessmelt Arctic sea ice: a) September extent ensemble mean 1850-2100 timeseries, b) March volume ensemble mean 1850-2100 timeseries, c) September extent ensemble mean 20-year trends, d) March volume ensemble mean trends. Grey shading shows 95% confidence intervals on trends calculated by bootstrapping CESM2-LE ensemble means with 4 members 1,000 times.

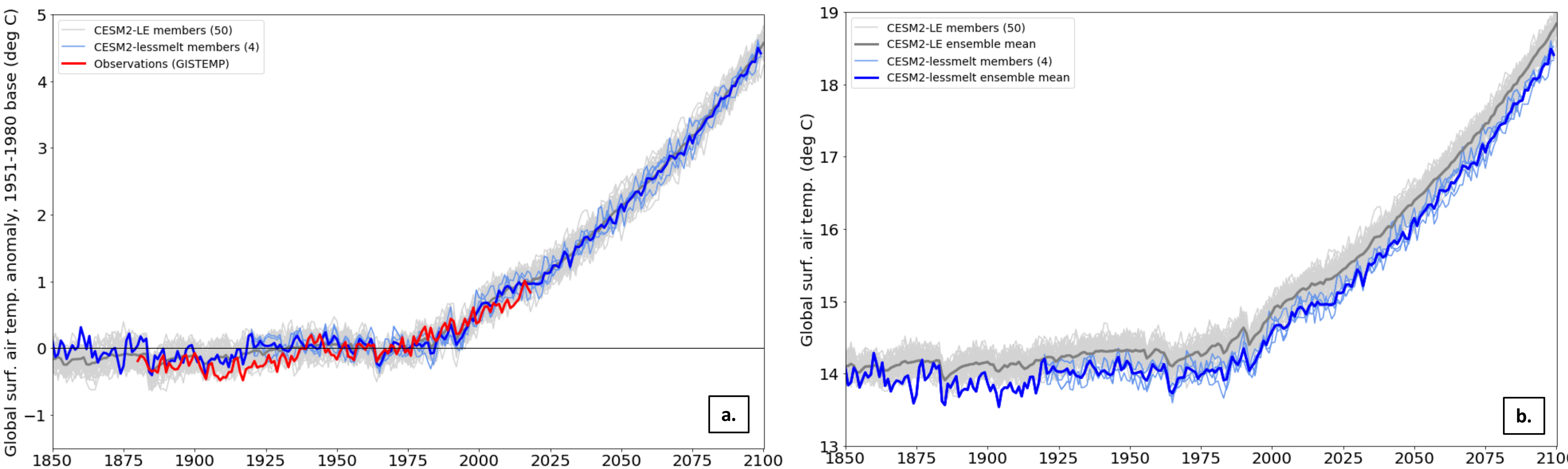

Figure 13. Transient evolution global annual mean surface air temperature in CESM2-LE and CESM2-lessmelt: a) anomaly from 1951-1980 with observations (GISTEMP, Hansen et al. 2010), b) absolute value

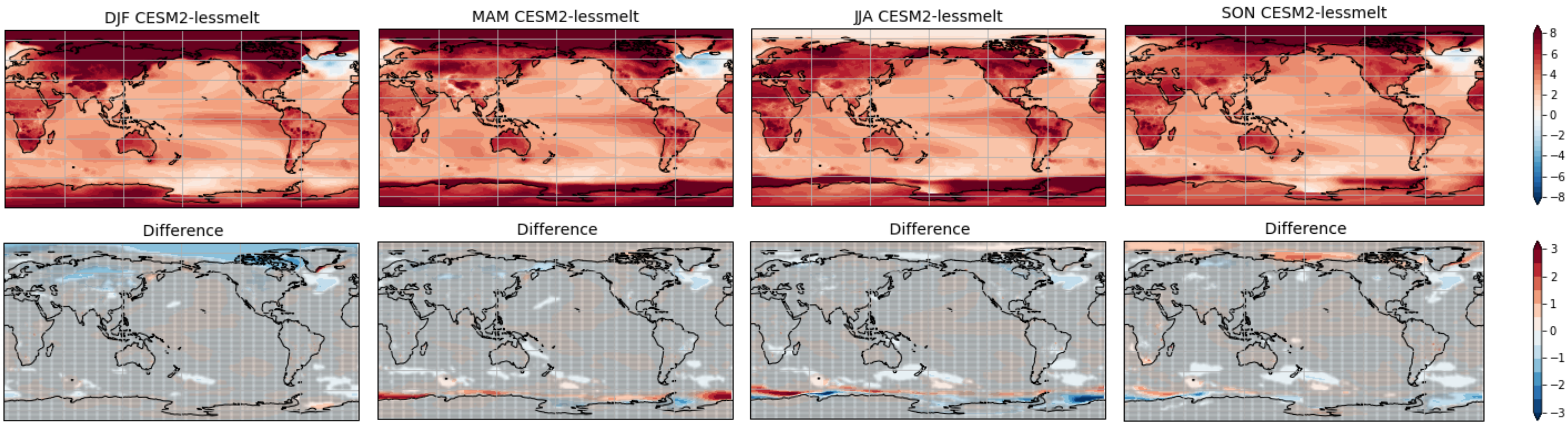

Figure 14. Ensemble mean surface temperature increase (2080-2099 minus 1920-1939) by season. Top row shows CESM2-lessmelt. Bottom row shows difference (CESM2-lessmelt minus CESM2-LE). Stippling indicates where differences between CESM2-lessmelt and CESM2-LE ensemble means are *not* statistically significant.

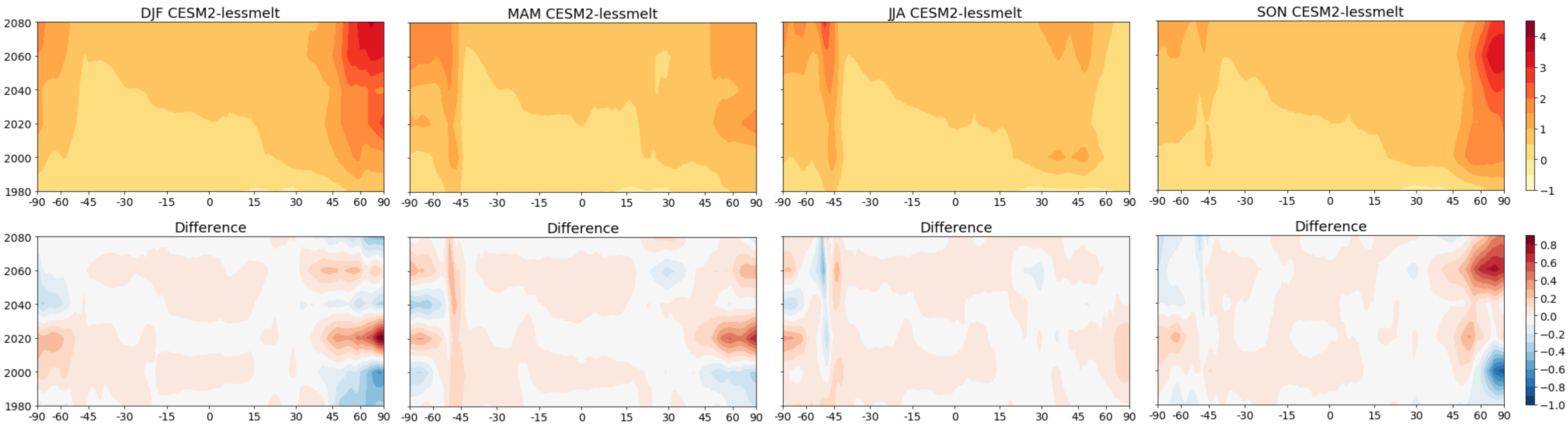

Figure 15. Zonal ensemble mean surface warming rates by season. Top row shows CESM2-lessmelt. Bottom row shows difference (CESM2-lessmelt minus CESM2-LE). Units of warming rate are K/20 years with the start year plotted on the vertical axis.